minerals

MDPI

Article

Control Mechanisms of Diagenetic Environment on Tight Sandstone Reservoir Quality: A Case Study of the Shaximiao Formation in the Sichuan Basin, China

Shengyu Li [1,2,*], Jingchun Tian [3,*] and Chao Luo [1,2]

[1] School of Petroleum Engineering, Chongqing University of Science and Technology, Chongqing 401331, China
[2] Chongqing Key Laboratory of Complex Oil and Gas Field Exploration and Development, Chongqing University of Science and Technology, Chongqing 401331, China
[3] Institute of Sedimentary Geology, Chengdu University of Technology, Chengdu 610059, China
* Correspondence: 2021005@cqust.edu.cn (S.L.); chdugeology@163.com (J.T.)

Abstract

The Shaximiao Formation in the Sichuan Basin possesses favorable exploration potential for unconventional oil and gas, whereas systematic studies on the genetic mechanism of its tight sandstone reservoirs remain insufficient. In this study, tight sandstones of the study area were comprehensively investigated through multiple analytical methods, including thin section observation, scanning electron microscopy, cathodoluminescence, electron probe microanalysis, fluid inclusion testing, and reservoir physical property measurement. The Shaximiao Formation belongs to typical low-permeability tight reservoirs, which are predominantly composed of lithic arkose, followed by feldspathic litharenite and arkose. A variety of authigenic minerals are widely developed in the reservoirs, including laumontite, calcite, quartz overgrowth, feldspar overgrowth, and clay minerals. The main reservoir spaces consist of primary pores, feldspar dissolution pores, and laumontite dissolution pores. The reservoirs have reached middle diagenetic stage A. A full set of diagenetic events can be identified in the study interval. These processes consist of gypsum cementation, chlorite cementation, feldspar dissolution, quartz overgrowth, kaolinite precipitation, laumontite cementation and dissolution, carbonate cementation, and pyrite cementation. Synthetic analysis of microscopic inclusion occurrences, homogenization temperature, and salinity data reveals that the Shaximiao Formation experienced three successive charging episodes of three different fluid endmembers, namely indigenous formation brine, organic acid fluid, and low-salinity surface-derived fluid. These multiphase mixed fluids sequentially altered authigenic minerals and pore spaces under variable open–closed diagenetic systems. The diagenetic system evolved progressively from an early closed environment dominated by laumontite precipitation to a middle–late semi-open-to-open environment dominated by calcite and siliceous cementation. Differential fluid migration controls diagenetic processes and the spatial distribution of cements, which fundamentally accounts for the strong heterogeneity of the reservoirs. Three types of diagenetic environments are classified in the study area, namely compaction-dominated, cementation-dominated, and dissolution-dominated environments, which jointly control the diagenetic assemblages and physical property evolution of the reservoirs. Compaction acts as the primary pore-reducing factor, causing a total porosity loss of 23.34%. Dissolution of feldspar and laumontite serves as the major pore-enhancing process, increasing the porosity by 5.26% and 4.32%, respectively. The mudstone and carbonate rock fragments in western Sichuan provide essential materials for calcite cementation, while intermediate-acid pyroclastics and plagioclase albitization collectively promote laumontite enrichment. The infiltration of meteoric freshwater and the upward migration of organic acids along faults induce feldspar

Check for updates

Academic Editor: Santanu Banerjee

Received: 11 May 2026
Revised: 27 June 2026
Accepted: 28 June 2026
Published: 6 July 2026

Copyright: © 2026 by the authors. Licensee MDPI, Basel, Switzerland. This article is an open access article distributed under the terms and conditions of the Creative Commons Attribution (CC BY) license.

dissolution, further resulting in the formation of kaolinite and quartz overgrowths. The brackish diagenetic environment under arid climatic conditions facilitates the development of early gypsum, which is finally transformed into anhydrite through burial dehydration.

Keywords: tight sandstone reservoir; diagenetic environment; reservoir characterization; Shaximiao Formation; Sichuan Basin

1. Introduction

Tight sandstone reservoirs, characterized by low porosity, low permeability, and strong heterogeneity, are critical targets for unconventional hydrocarbon exploration [1–5]. Their formation and evolution are controlled mainly by sedimentation, diagenesis, and tectonism. Correspondingly, primary, fractured, and secondary low-permeability reservoirs are dominated by sedimentary, tectonic, and diagenetic processes, respectively. In tight sandstones, diagenesis strongly controls reservoir densification, pore reconfiguration, and heterogeneous distribution. Variable bulk composition and divergent diagenetic pathways driven by sedimentary conditions and provenance further amplify reservoir differentiation, highlighting the necessity of clarifying differential diagenetic evolution.

In recent years, with the continuous development and refinement of various technical methods, substantial progress has been made in reservoir diagenesis research. Research approaches have evolved from qualitative to quantitative, and research content has shifted from macroscopic phenomenological analysis to microscopic mechanistic interpretation. A series of innovative insights have been achieved in the studies of reservoir temperature–pressure evolution, diagenetic fluid activities, system sealing properties, and dissolution–precipitation mechanisms of diagenetic minerals [6–10]. However, several controversies remain regarding the timing of diagenesis, system sealing properties, and the transformation and migration of diagenetic materials. Some scholars propose that the burial diagenetic environment is predominantly a closed system, in which diagenetic fluids cannot flow on a large scale, diagenetic mineral transformations follow the principle of mass balance, and diagenetic products are precipitated nearly in situ mainly via diffusion [11–13]. Other researchers argue that the burial diagenetic environment is still an open system, where diagenetic fluids can flow extensively through advection or convection, and diagenetic products can migrate over long distances, be effectively transported out of the reservoir, and precipitate in distant locations. Sedimentation lays the material foundation and initial physical properties of reservoirs. Different sedimentary microfacies control the distribution, grain size, sorting, and matrix content of sand bodies, and determine the development scale and spatial pattern of primary pores. Subsequent diagenesis continuously modifies reservoir spaces through compaction, cementation, and dissolution. Compaction greatly reduces primary pores, various cements block pore throats, and mineral dissolution creates secondary pores to improve reservoir quality. The combined evolution of sedimentation and diagenesis ultimately determines the overall quality and heterogeneity of reservoirs [14–19].

With expanding gas discoveries from the Middle Jurassic Shaximiao Formation in the Sichuan Basin [20–23], this interval has become a key target for tight sandstone research. Existing work mainly addresses sedimentary facies and sand body distribution, clarifying basic sedimentary and reservoir features. However, strong intralayer reservoir heterogeneity remains poorly explained, and regional differences in diagenetic environments and their controls on reservoir quality lack systematic analysis.

Focusing on the diagenetic environment, this study integrates petrological, mineralogical, and physical data to identify major diagenetic assemblages and sequences. It

further reveals how differentiated diagenetic conditions control pore evolution and reservoir sorting, supporting favorable reservoir prediction for practical tight gas exploration. This study proposes three key innovations. First, it systematically clarifies the genesis and material sources of the major diagenetic minerals and cements developed in the study area. Second, it reveals the constraining effects of arid climate and brackish water conditions on early diagenetic processes, which supplements and improves the understanding of the early diagenetic evolution of the Shaximiao Formation. Third, this study confirms that the differentiation of diagenetic environments dominates the heterogeneity of reservoir physical properties, establishes a reliable correlation between diagenetic conditions and reservoir quality, and provides a solid geological basis for the prediction of favorable tight gas reservoirs.

2. Geological Setting

The Sichuan Basin was formed by long-term combined tectonic movements affecting the Upper Yangtze Block during the evolution of the Tethyan tectonic domain, Qinling tectonic belt, and Circum-Pacific tectonic domain from the Indosinian to Himalayan periods [22]. Continental sediments were initially deposited in the Upper Yangtze region, and the prototype basin was subsequently modified by multi-stage and progressive compression, leading to the formation of the present structural basin during the Late Himalayan epoch (Figure 1a). At present, the basin is divided into five tectonic units: Western Sichuan, Central Sichuan, Northern Sichuan, Southern Sichuan, and Eastern Sichuan, corresponding to depression zones, uplift zones, low-steep structural belts, and high-steep structural belts, respectively. Central Sichuan is located between Longquan Mountain and Huaying Mountain, where Jurassic–Cretaceous strata are predominantly exposed. Western Sichuan encompasses the low-steep zone of the Western Sichuan Depression, the western part of the gentle zone of the Northern Sichuan Depression, and the northwestern corner of Central Sichuan, which is mainly covered by Quaternary deposits.

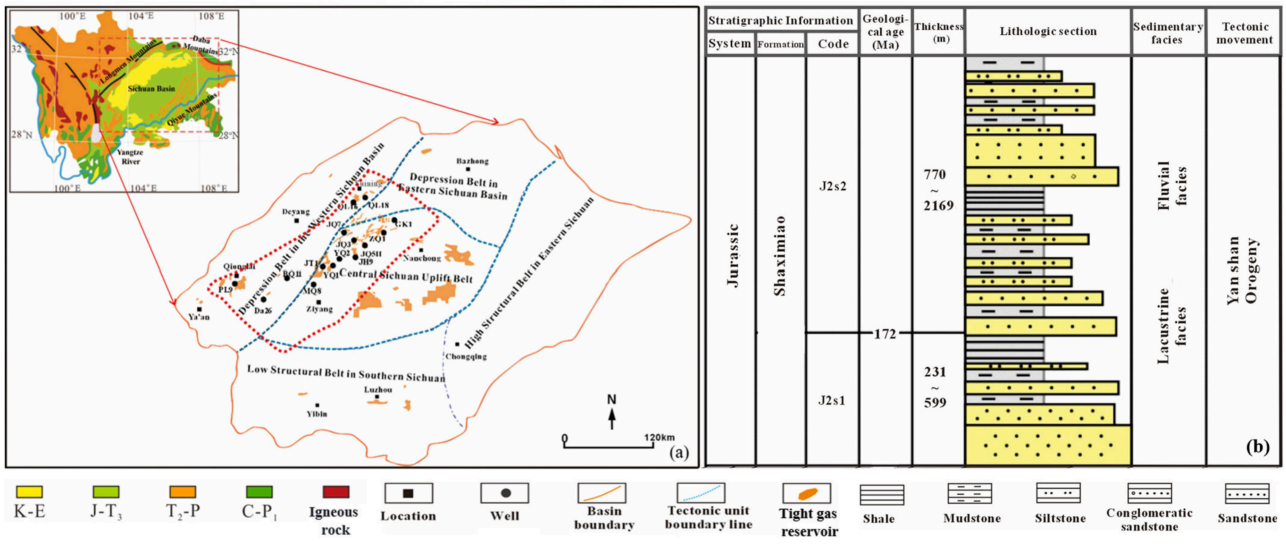


Figure 1. Geological background and stratigraphic characteristics of the study area in the Sichuan Basin, China. (**a**) Tectonic units and distribution of continental tight gas exploration discoveries in the Sichuan Basin [12]; (**b**) characteristics of continental sedimentary strata in the Sichuan Basin.

From the Sinian-to-Middle Triassic, the Sichuan Basin was dominated by marine sedimentation. Since the Middle–Late Triassic, the basin has entered a continental sedimentary stage characterized by terrigenous clastic rocks [20–23]. The Jurassic strata are mainly composed of clastic rocks deposited in inland freshwater lacustrine facies. The target strata

of this study, the Shaximiao Formation, belongs to the Middle Jurassic in the Sichuan Basin. It is characterized by an unequal-thickness interbedded sequence of sandstone and mudstone, with a total thickness ranging from 600 to 2400 m (Figure 1b).

3. Samples and Methods

In this study, representative core samples were collected from 15 typical wells in the central and western Sichuan Basin, including Qiulin 16, Qiulin 18, Pingluo 9, Yongqian 2, Baiqian 11, Da 26, Maqian 8, Yanqian 1, Zhongqian 1, Jiantan 1, Jinqian 7, Jinqian 3, Jinqian 5H, Jinhua 9, and Guankou 1. All sampling intervals are concentrated in the target tight sandstone strata of the study area. During sampling, core lithology, sedimentary structures, cement characteristics, and pore development features were firstly observed and recorded in detail. The sampling strategy strictly followed scientific principles: samples were collected away from sand–mud contact boundaries and erosion surfaces, and cores with special sedimentary and diagenetic phenomena were preferentially selected to ensure the representativeness and typicality of experimental samples. Among them, fluid inclusion samples were specifically obtained from Jinqian 7 and Maqian 7; electron probe microanalysis (EPMA) samples were collected from Guankou 1, Jiantan 1, and Jinqian 7; and cathodoluminescence (CL) test samples were screened from Jinqian 7, covering the key wells of the study area and meeting the requirements of systematic diagenetic characteristic analysis.

Multiple systematic petrological and geochemical tests were carried out in this study to clarify the petrological characteristics, diagenetic processes, and reservoir evolution mechanisms, and the detailed experimental principles and procedures are as follows.

(1) Standard thin sections were prepared for all core samples and observed systematically using a Leica DM4500P polarizing microscope (Leica Microsystems, Wetzlar, Germany) and a JSM-7900F field emission scanning electron microscope (FE-SEM, JEOL, Tokyo, Japan) [24,25]. The porosity and permeability measurements of core samples in this study were conducted using the CMS-300 fully automated overburden porosity-permeability instrument (Core Laboratories, Huston, TX, USA) [26]. Under plane-polarized and cross-polarized light, we quantitatively and qualitatively identified mineral composition, grain contact relationships, cement types and content, pore types, and planar porosity. Special attention was paid to typical diagenetic phenomena, including the filling characteristics of calcite, chlorite, and laumontite cements, feldspar albitization and dissolution, and the transformation and spatial distribution of clay minerals. FE-SEM was further used to observe nanoscale pore structures, micro-pore throats, and microscopic mineral morphological characteristics, which compensates for the limitation of optical microscopy in identifying fine diagenetic features.

(2) X-ray diffraction clay mineral analysis was performed on all samples to quantitatively determine the relative contents of illite, kaolinite, chlorite, and illite/smectite mixed-layer clay minerals [27]. Based on the diffraction peak characteristics and spectral matching principles, the types and proportions of clay minerals were accurately identified, which clarifies the clay mineral assemblage characteristics and provides basic data for analyzing clay mineral-controlled reservoir densification and pore evolution.

(3) Cathodoluminescence tests were conducted on selected samples from the Jinqian 7 well. The basic principle is that different mineral components and trace element contents produce distinct luminescence colors and intensities under electron beam excitation. This technique can effectively distinguish multi-stage cementation, identify the growth sequence of quartz and calcite cements, and accurately characterize

the superimposed transformation characteristics of multi-period diagenetic fluids, which is crucial for determining the diagenetic evolution sequence of tight sandstone reservoirs [28].

(4) Electron probe microanalysis was carried out on samples from Guankou 1, Jiantan 1, and Jinqian 7 wells. By detecting the characteristic X-ray signals of micro-area minerals, this method realizes the in situ quantitative analysis of major and trace element compositions of feldspar, laumontite, carbonate cements, and clay minerals [26]. It can effectively identify mineral alteration, element migration, and metasomatic diagenesis, and further reveal the material basis and geochemical mechanism of dissolution and cementation in the study area.

(5) To constrain the diagenetic temperature–pressure conditions and paleofluid properties, systematic fluid inclusion analysis was performed on samples from typical wells. Primary and secondary fluid inclusions hosted in quartz and calcite cements were screened under a polarizing microscope. A Linkam THMS600 (Linkam Scientific Instruments, Surrey, UK) heating–cooling stage was used for microthermometric testing to obtain homogenization temperature (Th) and ice-melting temperature (Tm). Fluid salinity was further calculated based on the ice-melting temperature formula [29,30]. Meanwhile, a Renishaw inVia laser Raman spectrometer was adopted to qualitatively analyze the gas–liquid composition of individual fluid inclusions, identifying major components including H_2O, CO_2, and CH_4. These fluid inclusion data provide reliable temperature and salinity parameters for dividing diagenetic stages, defining diagenetic timing, and reconstructing the paleofluid evolution of tight sandstone reservoirs.

This work is supported by the project Sedimentary and Reservoir Evolution of the Shaximiao Formation in the Sichuan Basin from PetroChina Southwest Oil and Gasfield Company, and has been updated with new analytical data obtained in this research. All single-factor histograms, lithology-physical property crossplots, and mineral composition ternary diagrams in this study were plotted using OriginPro 2023, and then uniformly formatted and polished with CorelDRAW 2020.

4. Results

4.1. Petrological Characteristics

Sandstone classification is conducted based on the QFL ternary diagram [31,32]. Point counting data of thin sections indicate that feldspar content is generally higher than lithic fragment content, so lithic arkose dominates the Shaximiao Formation Reservoirs. The results of sandstone triangular plotting show that the average content of quartz (Q) end-member is 42.7%, feldspar (F) end-member is 32.5%, and lithic (R) end-member is 24.8%. Among the lithic fragments, metamorphic and sedimentary rock fragments are dominant, with minor igneous rock fragments (Figure 2).

XRD whole-rock diffraction analysis indicates that quartz is the most abundant mineral in the Shaximiao sandstones, followed by plagioclase and clay minerals, with minor amounts of calcite, orthoclase, and analcime, which is consistent with the results of thin-section petrographic analysis (Figure 3). Thin-section microscopic examination reveals that the average content of carbonate cement in the Shaximiao Formation sandstones is 4.19%, and the average content of argillaceous material is 7.63%.

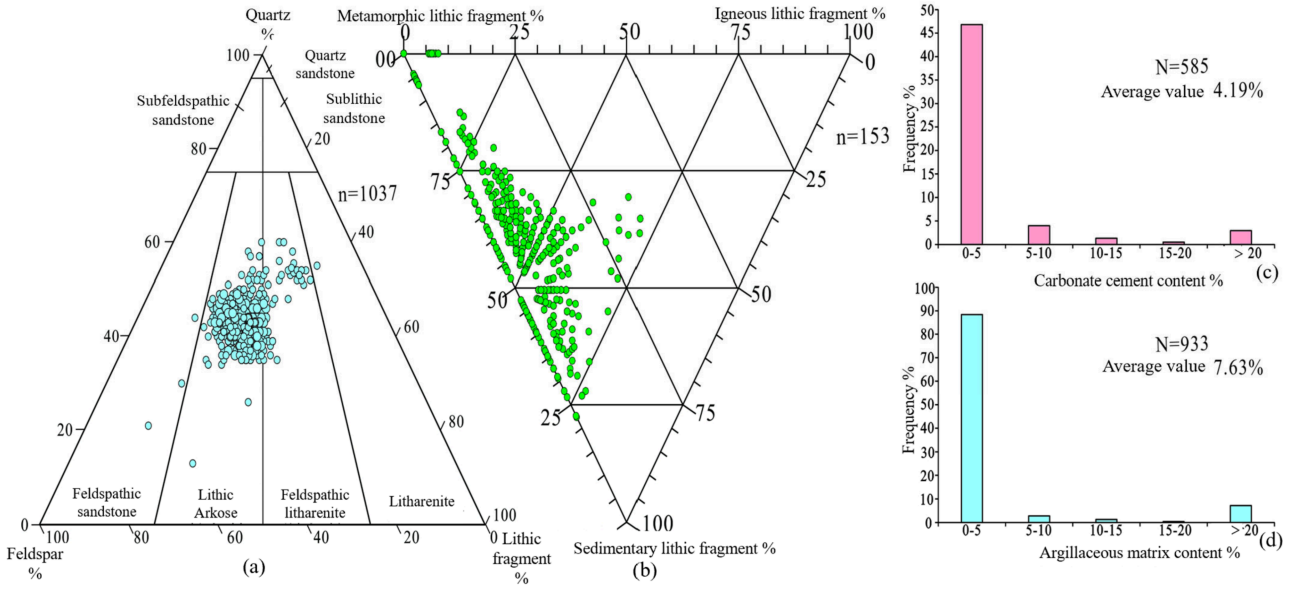


Figure 2. Ternary plots and histograms of main interstitial fillings in the Shaximiao Formation. The sandstone classification in this study follows the QFL triangular diagram [31,32]. (**a**) QFL ternary diagram for sandstone classification; (**b**) Ternary diagram of metamorphic, igneous and sedimentary lithic fragment components; (**c**) Frequency distribution histogram of carbonate cement content; (**d**) Frequency distribution histogram of argillaceous matrix content.

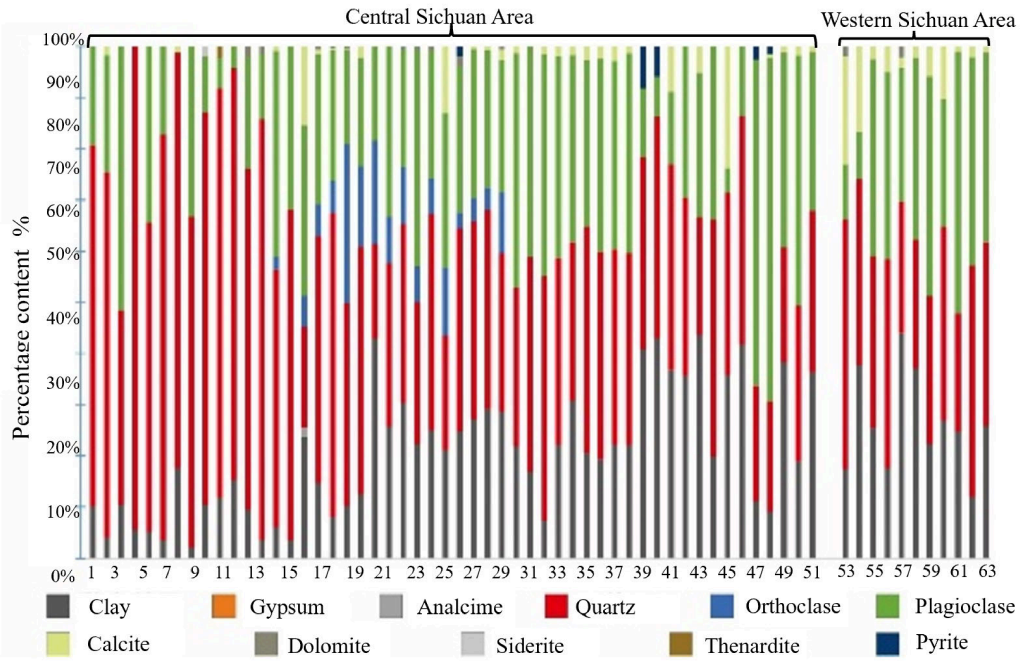


Figure 3. Whole-rock mineral composition of sandstones in the Shaximiao Formation.

4.2. Main Diagenetic Processes

4.2.1. Characteristics of Mechanical Compaction

The reservoirs of the Shaximiao Formation, generally buried at depths less than 3000 m, exhibit a moderate overall compaction intensity. In the tight sandstone reservoirs of the Shaximiao Formation in central Sichuan, compaction is primarily characterized by point-line contacts between grains (Figure 4).

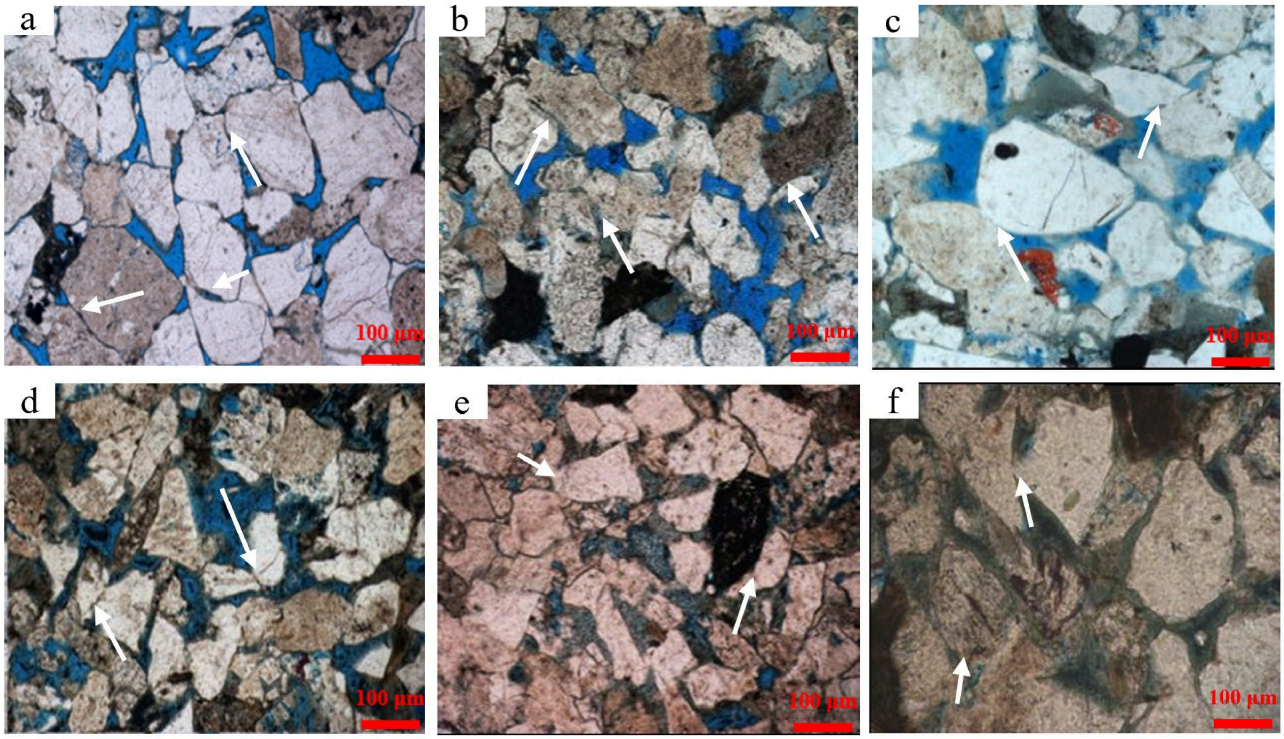


Figure 4. Typical microphotographs of compaction in the Shaximiao Formation Reservoirs. (**a**) Well Jinhua 9, 2224.06 m, line contact; (**b**) Well Jinqian 5H, 2148.67 m, point-line contact; (**c**) Well Jinqian 3, 2153.07 m, point-line contact; (**d**) Well Da 21, 1239.15 m, point-line contact; (**e**) Well Baiqian 11, 2091.39 m, point-line contact; (**f**) Well Pingluo 9, 1991.21 m, line contact.

Combined with the tectonic evolution background and sedimentary characteristics of the central Sichuan uplift belt in the study area, the formation of this moderate-intensity compaction is jointly controlled by burial rate, sediment grain size, and argillaceous content. Its microscopic manifestations and impacts on the reservoir exhibit significant regional characteristics.

4.2.2. Types and Characteristics of Authigenic Cementation

Calcite cement is the most abundant cement in the Shaximiao Formation sandstones (Figure 5a). It mainly fills intergranular pores and generally develops in at least one stage. The content of early calcite ranges from 2% to 12%, and it mostly occurs as fine-to-medium crystalline poikilitic aggregates. Authigenic siliceous cement is widely developed (Figure 5b), including quartz secondary overgrowths and authigenic quartz. Quartz secondary overgrowths form along quartz grain margins. Clay films exist at boundaries between overgrowths and host grains, which commonly lead to concavo–convex contacts among quartz grains. Authigenic quartz occurs as euhedral granular crystals and fills intergranular and intragranular dissolved pores. Authigenic feldspar is also present in the sandstones and grows dominantly along feldspar grain margins (Figure 5b). Compared with host feldspar grains, authigenic feldspar features clean surfaces with no evident clay mineral alteration, and is dominated by albite.

Laumontite cement mainly occurs in the central Sichuan Basin (Figure 5c), with a content of 5%–8% and a maximum of 18%. Laumontite precipitated in the early diagenetic stage and generally occurs as poikilitic cement, with a much more limited distribution than early calcite cement. Partial dissolution of laumontite is observed in thin sections, forming intercrystalline pores. It forms via the alteration of acidic volcanic rock debris in alkaline

formation water. Elements including silicon, aluminum, and calcium released from the debris reprecipitate within sandstone pores to generate laumontite cement.

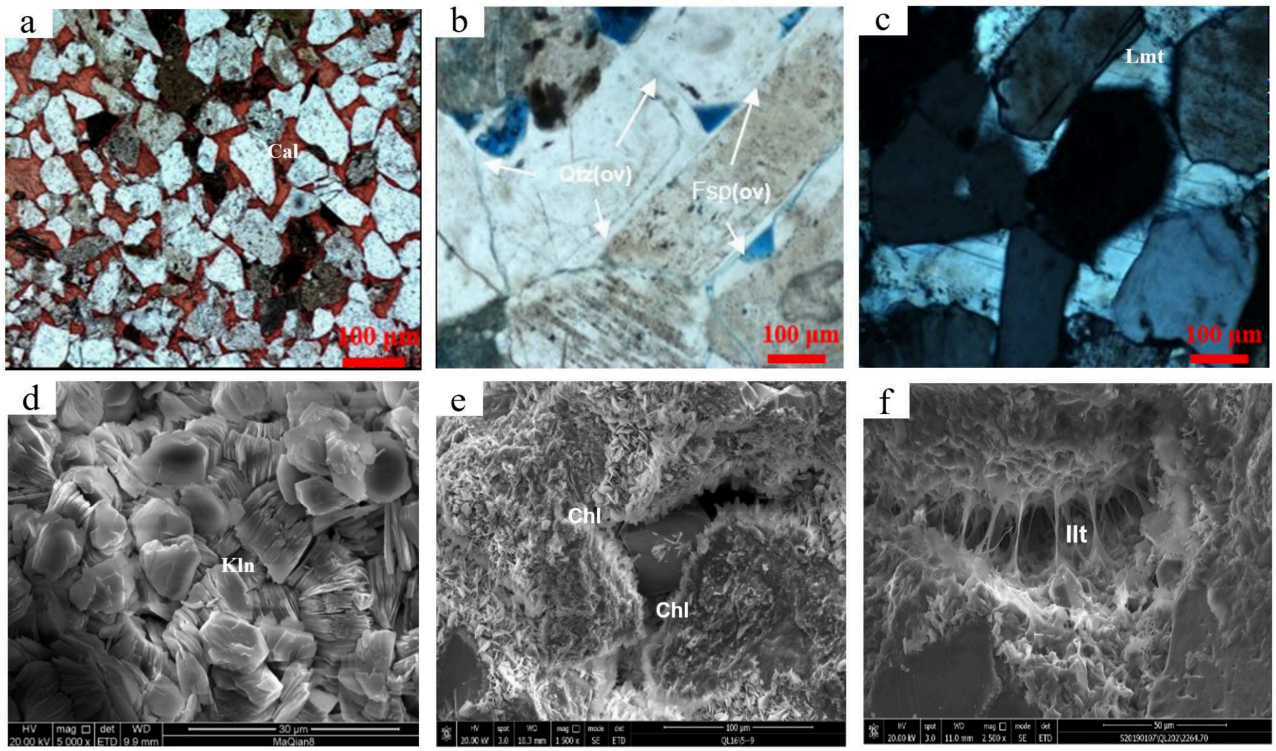


Figure 5. Typical microphotographs of cementation in the Shaximiao Formation Reservoirs. (**a**) Well Jinqian 5H, 1950.19 m, calcite cementation; (**b**) Well Jinqian 3, 2148.8 m, quartz overgrowth and feldspar overgrowth; (**c**) Well Jinqian 3, 2149.65 m, laumontite cementation; (**d**) Well Maqian 8, 1877.52 m. Book-shaped kaolinite crystals abundantly fill intergranular pores (SEM). Explanations for the bottom parameters: HV 20.00 kV refers to an electron beam accelerating voltage of 20 kilovolts; mag 5000 × denotes a magnification of 5000 times; det ETD stands for Everhart-Thornley secondary electron detector; WD 9.9 mm represents the working distance of 9.9 mm between the objective lens and the sample. The scale bar at the bottom corresponds to 30 μm, and MaQian8 is the core sample number; (**e**) Well Qiulin 16, 2411.24 m. Chlorite develops as grain-coating rims on particle surfaces (SEM). Explanations for the bottom parameters: HV 20.00 kV is the accelerating voltage of 20 kilovolts; spot 3.0 indicates the electron beam spot size grade; WD 10.3 mm means a working distance of 10.3 mm; mag 1500 × represents a magnification of 1500 times; mode SE denotes secondary electron imaging mode; det ETD is the secondary electron detector. The bottom scale bar equals 100 μm, and QL16/5-9 is the core sample number; (**f**) Well Qiulin 202, 2264.7 m. Filamentous illite grows in a bridging pattern within pores (SEM). Explanations for the bottom parameters: HV 20.00 kV is the accelerating voltage of 20 kilovolts; spot 3.0 refers to the electron beam spot size grade; WD 11.0 mm stands for a working distance of 11 mm; mag 2500 × indicates a magnification of 2500 times; mode SE represents secondary electron imaging mode; det ETD is the secondary electron detector. The scale bar at the bottom corresponds to 50 μm, and S20190107/QL202/2264.70 is the core sampling number. Calcite—Cal, quartz—Qtz, quartz overgrowth—Qtz(ov), feldspar—Fsp, feldspar overgrowth—Fsp(ov), Illite—Ilt, laumontite—Lmt, Chlorite—Chl, kaolinite—Kln.

Clay minerals in the study area are dominated by kaolinite, chlorite, and illite (Figure 5d–f). Kaolinite occurs as book-like or vermicular aggregates in intergranular and intragranular pores, with abundant tiny intercrystalline micropores developed within the aggregates. Two types of chlorite are identified in the reservoir. Grain-coating chlorite forms in the early diagenetic stage, exhibiting scaly or petal morphologies with a thickness of 3.0–6.0 μm, and rarely extends deeply into pore spaces. This chlorite forms prior to significant porosity reduction by mechanical compaction and is closely associated with strong hydrodynamic conditions. With increasing

burial depth and formation temperature, intergranular filling chlorite gradually develops. It displays more complete crystal morphologies than early-stage chlorite, with poor continuity but strong aggregation within pores. Illite exhibits variable morphologies, mainly filamentous, platy, and bridge-like, with minor honeycomb aggregates. It commonly coexists with other interstitial components, showing wide distribution but poor continuity. Illite is predominantly derived from the transformation of sedimentary components and matrix, and fluid activities facilitate illite precipitation from interstitial materials.

4.2.3. Types and Characteristics of Mineral Dissolution

Dissolution in the study area is dominated by feldspar and laumontite dissolution. They differ microscopically, govern pore development, and are key indicators for diagenetic environment discrimination.

K-feldspar and plagioclase both show obvious selective dissolution (Figure 6a). K-feldspar is pervaded by intragranular dissolved pores and moldic pores rimmed with kaolinite. Plagioclase is less intensely dissolved, producing small pits and fractures, with illite as the principal accessory mineral.

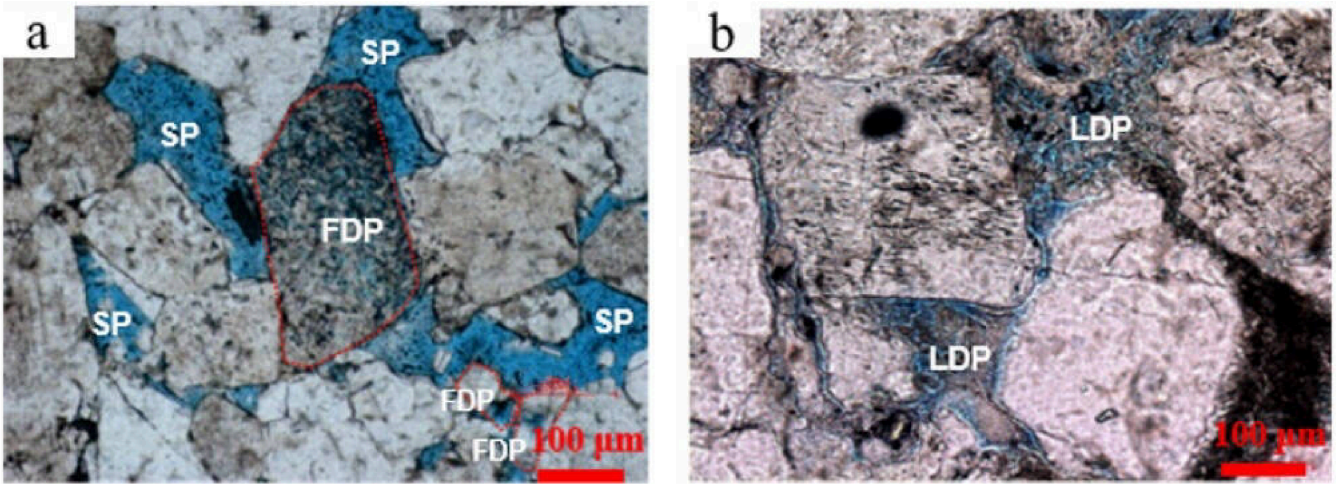


Figure 6. Typical microphotographs of dissolution in the Shaximiao Formation Reservoirs. (**a**) Well Qiulin18, 2095.27 m, secondary dissolution pores and feldspar dissolution pores; (**b**) Well Jinqian 7, 1758.65 m, laumontite dissolution pores. Secondary dissolution pores—SP, feldspar dissolution pores—FDP, laumontite dissolution pores—LDP.

Laumontite dissolution is a typical paragenetic alteration in tight sandstones, chiefly found in fine-to-medium grained sandstones (Figure 6b). Occurring as basal intergranular cement, laumontite is altered by late acidic fluids to form polygonal pores and fracture networks, creating effective reservoir spaces.

4.2.4. Types and Characteristics of Mineral Replacement

Replacement constitutes a key diagenetic process for Shaximiao Formation reservoirs in central Sichuan and predominantly occurs in six modes: calcite replacement of laumontite, feldspar, and chlorite, alongside kaolinite replacement of calcite and feldspar, plus calcite replacement of kaolinite (Figure 7a–c,f). These replacement varieties feature prominent discrepancies in microscopic features, development intensity, and regulatory impacts on reservoir porosity. Calcite-replacing laumontite is the most extensively developed and forms under conditions of limited laumontite dissolution, characterized by gradational replacement margins and remnant mineral textures. In addition, calcite may

replace feldspar along intragranular dissolution pores and microfractures, or substitute pre-existing chlorite within chlorite grain coatings and cementation zones.

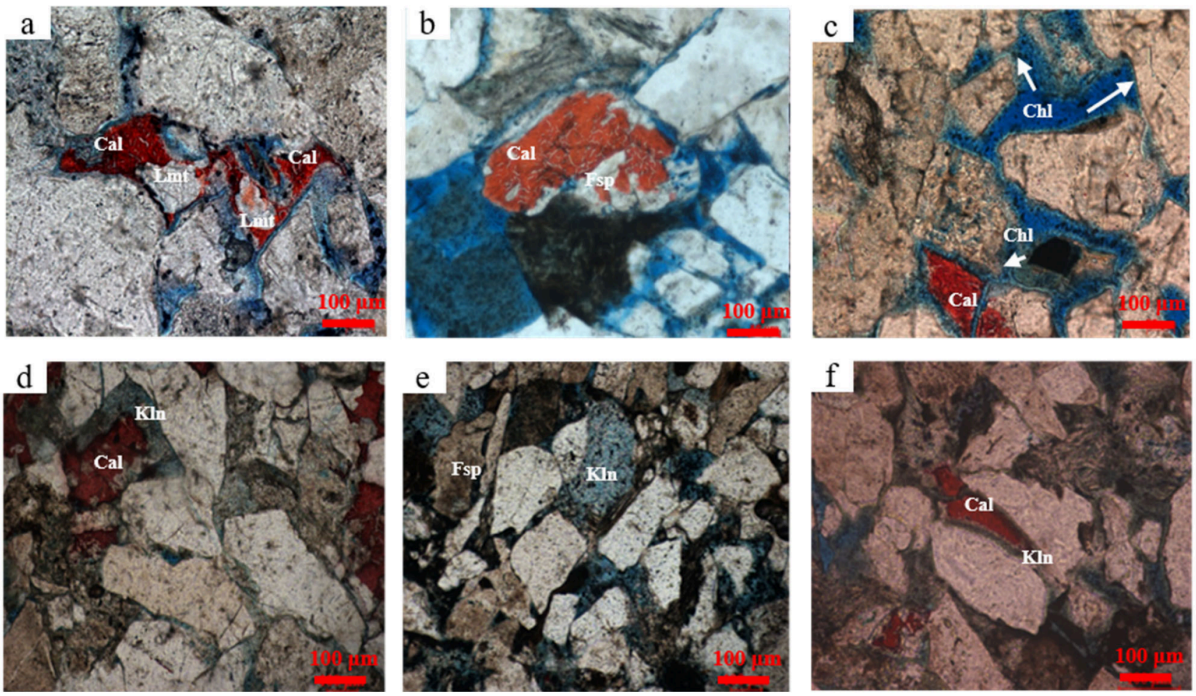


Figure 7. Typical microphotographs showing replacement in the Shaximiao Formation Reservoirs. (**a**) Well Jinqian 7, 1758.65 m, calcite replacing laumontite; (**b**) Well Jinqian 3, 2149.65 m, calcite-replacing feldspar; (**c**) Well Qiulin 16, 2411.24 m, calcite-replacing chlorite; (**d**) Well Maqian 8, 1872.10 m, kaolinite-replacing calcite; (**e**) Well Yanqian 1, 1681.23 m, kaolinite-replacing feldspar; (**f**) Well Da 26, 1254.70 m, calcite-replacing kaolinite. Calcite—Cal, quartz—Qtz, quartz overgrowth—Qtz(ov), feldspar—Fsp, laumontite—Lmt, chlorite—Chl, kaolinite—Kln.

Kaolinite originates from feldspar dissolution and progressively replaces pre-existing calcite to form irregular replacement boundaries, yielding book-like or vermicular aggregates encased by residual calcite. Coeval with feldspar dissolution, kaolinite partially or completely replaces feldspar and occurs either within mineral grains or along grain margins. Furthermore, late-stage calcite obliterates primary book-like kaolinite aggregates via cross-cutting replacement (Figure 7d,e).

4.3. Reservoir Petrophysical Characteristics

The Shaximiao Formation Reservoirs in the central Sichuan Basin are typical low-permeability tight reservoirs (Figures 8 and 9). Variations in sandstone porosity and permeability with depth show that porosity generally decreases with increasing burial depth, while permeability changes slightly. Among 2617 sandstone samples from the Shaximiao Formation in central Sichuan, porosity peaks in the range of 12%–14%, accounting for 26% of the total samples, followed by 10%–12%, accounting for 25%. Approximately 50% of the samples have permeability lower than 0.2×10^{-3} μm^2, and more than 10% of the samples have permeability ranging from 1×10^{-3} μm^2 to 5×10^{-3} μm^2.

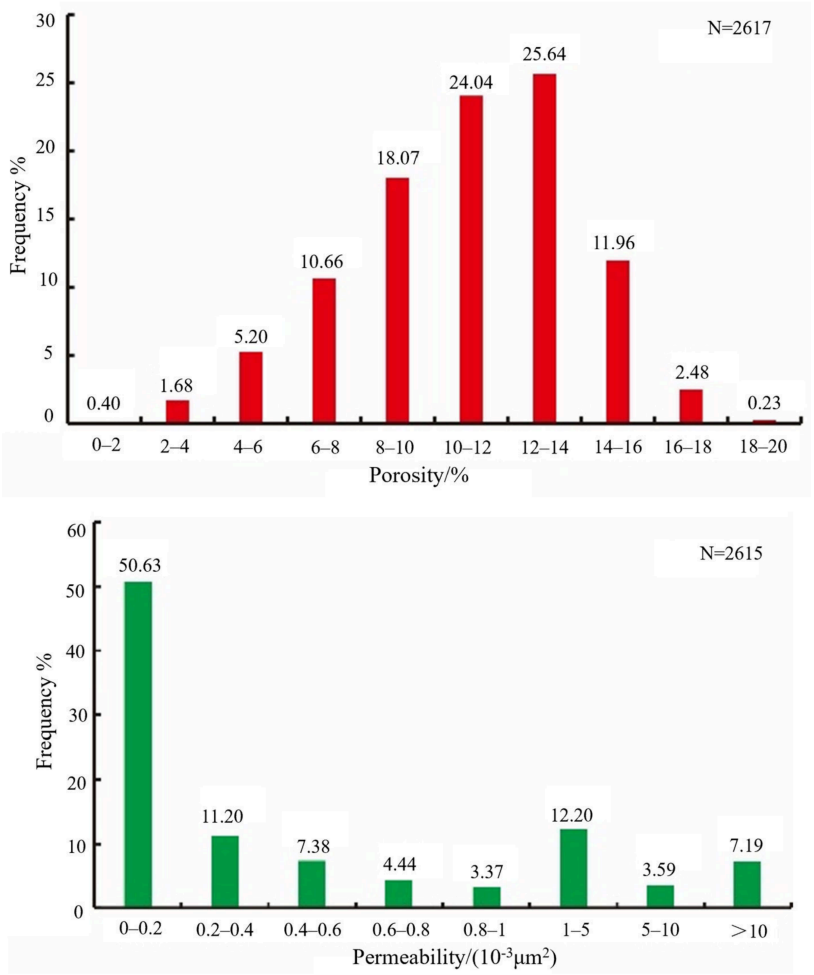


Figure 8. Histograms of porosity and permeability distribution in the Shaximiao Formation Reservoirs.

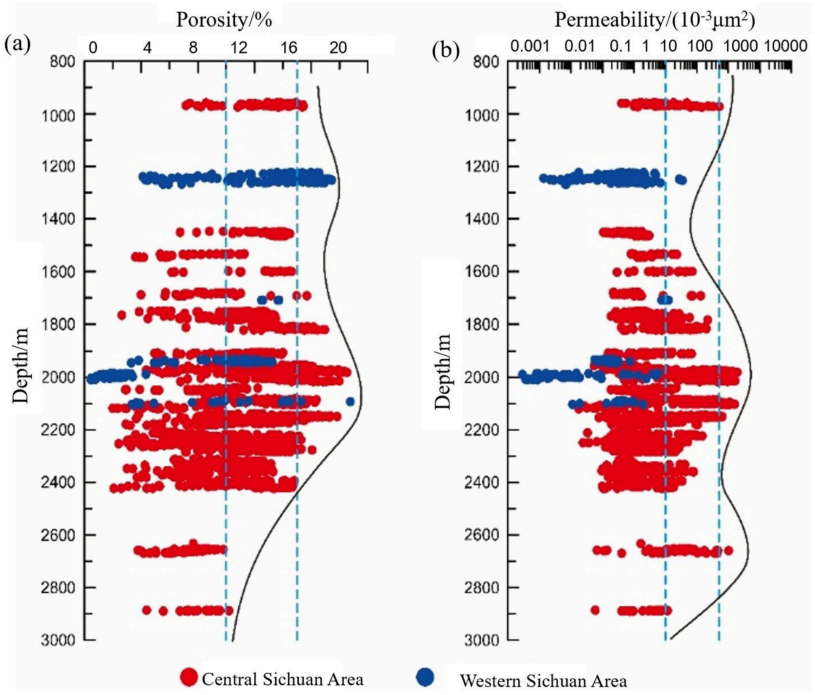


Figure 9. Porosity and permeability distribution of reservoirs in the Shaximiao Formation. (**a**) Vertical variation of porosity with burial depth; (**b**) Vertical variation of permeability with burial depth.

The differences in reservoir physical properties are essentially controlled by diagenetic fluid activities and the dynamic evolution of diagenetic environments. The overall decrease in porosity with increasing burial depth indicates that the diagenetic system transitions from a semi-open to open state during shallow burial to a closed state during deep burial. In the shallow burial stage, low-salinity surface-derived fluids and organic acids produced during hydrocarbon maturation infiltrated the reservoir and dissolved soluble minerals including feldspar, forming abundant secondary pores and creating the porosity peak ranging from 10% to 14%. As burial depth increases, the diagenetic system gradually becomes closed and fluid exchange weakens. Siliceous, calcareous, and other cements extensively precipitate within pores, occupying and compressing pore space and consequently reducing porosity continuously.

Figure 8 shows histograms of porosity and permeability distribution in the Shaximiao Formation Reservoirs.

The generally low permeability and the occurrence of local high-permeability zones reflect the heterogeneous migration of diagenetic fluids. Most reservoir intervals exist in a relatively closed environment with limited fluid activity. Fluids mainly migrate via in situ diffusion, and cements uniformly fill pore throats, resulting in permeability values generally lower than 0.2×10^{-3} μm^2. In areas with dominant fluid pathways formed by fractures and interconnected sand bodies, fluids migrate directionally for a long period. Continuous dissolution modifies pore throats and greatly improves pore connectivity, forming local high-permeability zones with permeability between 1×10^{-3} μm^2 and 5×10^{-3} μm^2. The asynchronous variation between porosity and permeability further demonstrates that diagenetic fluids exert differential impacts on pores and pore throats. Porosity is primarily governed by regional dissolution and cementation, while permeability depends largely on the development of fluid migration pathways. These factors collectively lead to strong reservoir heterogeneity, which is characterized by predominantly medium porosity and low permeability alongside local zones with relatively good petrophysical quality.

4.4. Characteristics of Diagenetic Fluids Based on Fluid Inclusions

The fluid inclusions in sandstones of the Shaximiao Formation are mostly round to oval in shape, with long-axis diameters mainly ranging from 2 μm to 8 μm (Figure 10a–c). They are dominated by liquid-rich gas–liquid two-phase inclusions and pure liquid inclusions, with a gas–liquid ratio of 5%–15%. According to fluid inclusion geochemistry criteria, only fluid inclusion assemblages trapped synchronously along mineral growth zonation, rather than post-crystallization microfractures, can be identified as primary inclusions. Inclusions distributed along transgranular fractures formed after mineral crystallization are defined as secondary inclusions and excluded from all subsequent temperature and salinity statistics in this study. The occurrence characteristics of inclusions vary significantly among different cement types, recording distinct fluid migration behaviors during diagenesis [5,7,33]. In siliceous cements, inclusions are widely developed and mostly arranged in bead-like chains with a small number of isolated individuals, reflecting directional fluid migration along pore throats during quartz precipitation prior to the development of late microfractures (Figure 10a). These bead-like chains strictly follow the growth lamellae of quartz overgrowth rims and never cut across crystal boundaries, which represent classic petrographic evidence for primary fluid inclusion assemblages trapped coevally with quartz crystallization. In contrast, calcite and laumontite cements host fewer inclusions that are mostly isolated, which indicates weak fluid activity and negligible directional flow during mineral precipitation (Figure 10b,c). These isolated inclusions are completely enclosed within intact mineral crystals and do not occupy late microcracks. We interpret these as likely primary fluid inclusion assemblages formed synchronously with mineral growth,

rather than secondary fracture-bound inclusions, though their isolated occurrence lacks sufficient petrographic context to confirm their origin with absolute certainty.

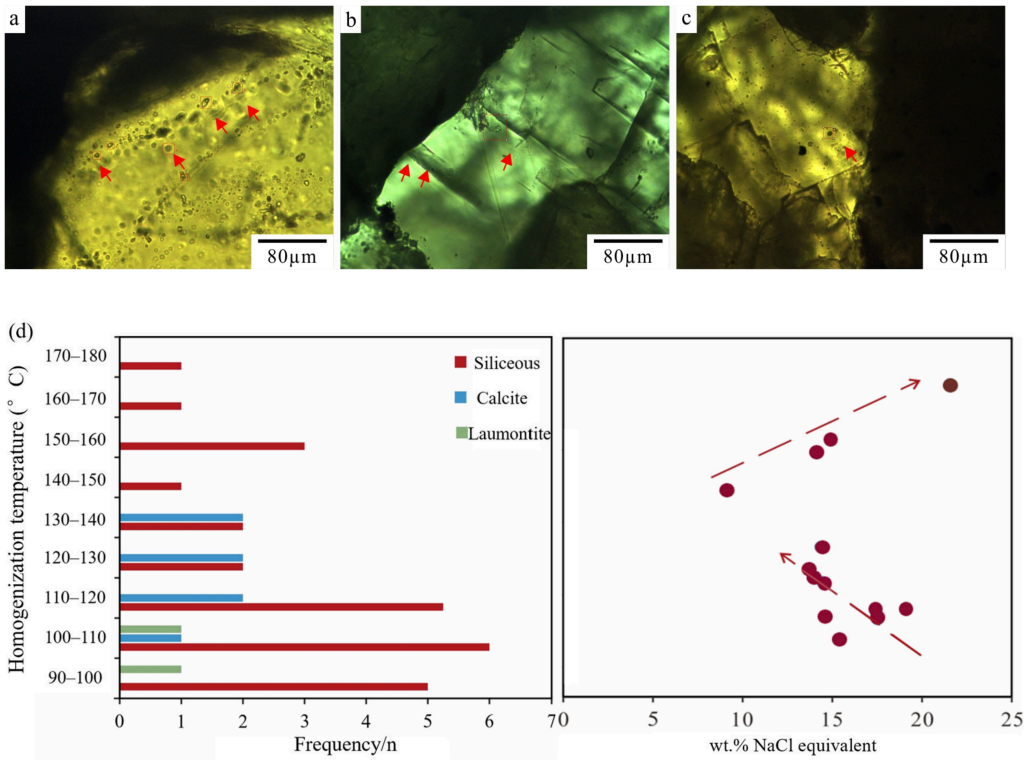


Figure 10. Microscopic characteristics and homogenization temperatures of fluid inclusions in cements of the Shaximiao Formation sandstones. (**a**) Well Maqian7, 1872.10 m, beaded siliceous cement; (**b**) Well Jinqian7, 1590.19 m, calcite cement; (**c**) Well Jinqian7, 974.50 m, laumontite cement; (**d**) **left**: histogram of homogenization temperature frequency for fluid inclusions in siliceous (red), calcite (blue), and laumontite (green) authigenic cements; **right**: cross-plot of homogenization temperature versus NaCl-equivalent salinity only for siliceous-hosted fluid inclusions. Reliable ice-melting temperature data cannot be obtained for calcite and laumontite inclusions due to their ultra-small size, so salinity values of these two cement types are unavailable and not plotted. The siliceous fluid data show two distinct evolutionary trends, revealing two stages of diagenetic fluid influx as described in the main text. For microthermometry, 3–6 primary fluid inclusions were measured from each FIA; 12 siliceous FIAs obtained full temperature–salinity data, while calcite and laumontite FIAs lack measurable ice-melting temperatures for salinity calculation.

To ensure the representativeness of microthermometric data, we followed standard fluid inclusion geochemistry protocols and measured 3–6 intact primary two-phase inclusions from each independent fluid inclusion assemblage (FIA): Siliceous cement: well-developed bead-like primary FIAs contain abundant large-sized fluid inclusions. We tested 4–6 inclusions per FIA, and a total of 12 FIAs yielded complete homogenization temperature and ice-melting temperature datasets for temperature–salinity cross-plotting. Calcite cement: primary isolated inclusions are sparse and tiny; 3–4 inclusions were measured for each FIA to obtain homogenization temperatures, yet stable ice-melting signals could not be detected for salinity calculation. Laumontite cement: valid primary FIAs are limited; 3 inclusions were tested for each available FIA; ultra-small inclusion volume prevented reliable ice-melting temperature measurement, so salinity data are unavailable.

All homogenization temperature and salinity data discussed below are exclusively derived from primary fluid inclusion assemblages identified by microscopic petrography, so the temperature–salinity sequences can reliably record the relative timing of diagenetic fluid evolution (Figure 10d). Homogenization temperature and salinity data of primary

fluid inclusions hosted in separate generations of authigenic cements record three distinct stages of diagenetic fluids with different geochemical characteristics [29,30,33–35]. The laumontite cements yield homogenization temperatures of 92–103.2 °C with a narrow distribution and stable salinity, indicating no obvious external fluid disturbance. The narrow and stable salinity range further proves that these primary inclusions have not been overprinted by later secondary fluids. This represents the earliest diagenetic fluid, which originated from indigenous formation brine within a relatively closed diagenetic system, where diagenetic materials precipitated mainly through in situ diffusion without long-distance migration. Calcite cements show homogenization temperatures of 108.7–135.9 °C (average 122.2 °C), overlapping with the low-temperature interval of siliceous cements and indicating contemporaneous fluid activity. The homogenization temperatures of siliceous cements range from 94.4 °C to 174.8 °C (average 121.2 °C) and exhibit an obvious bimodal distribution, which can be divided into an early low-temperature stage (100–110 °C) and a late high-temperature stage (150–160 °C). The early precipitation temperature is consistent with the temperature range of organic acid generation during hydrocarbon maturation (80–120 °C), confirming that the early fluid was a mixture of organic acid fluid and indigenous formation brine. The salinity of siliceous cement inclusions varies from 9.08 to 21.61 wt% NaCl equivalent and presents a trend of decreasing first and then increasing with rising temperature. The salinity decline at low temperatures indicates the mixing of low-salinity meteoric freshwater into primary formation fluids, which transformed the early closed system into a semi-open to open system. In this stage, fluids migrated directionally along connected sand bodies and fractures and promoted material transportation and enrichment. During the late high-temperature stage, the impact of low-salinity surface-derived fluids faded away, fluid salinity rose and recovered the geochemical signature of high-salinity indigenous formation brine, and the system evolved into a semi-open state dominated by limited local fluid–rock mass exchange.

For the synthetic analysis of microscopic inclusion occurrences, homogenization temperature and salinity data reveal that the Shaximiao Formation experienced three successive charging episodes of three different fluid endmembers, namely indigenous formation brine, organic acid fluid, and low-salinity surface-derived fluid. The diagenetic system presents a progressive evolutionary trend, changing from an early closed environment dominated by laumontite precipitation to a middle–late semi-open-to-open environment dominated by calcite and siliceous cementation. The differences in fluid sources, migration pathways, and material migration scales at various diagenetic stages control the diversity of diagenetic processes and the heterogeneous distribution of cements. This fluid-driven genetic mechanism fundamentally accounts for the strong intra-reservoir heterogeneity of the Shaximiao Formation sandstones and provides a critical basis for diagenetic environment classification and differential reservoir evolution analysis.

5. Discussion

5.1. Classification and Types of Diagenetic Environments

The occurrence relationship of authigenic minerals, which reflects their formation sequence, is the basis for studying diagenetic evolution. The relative timing of diagenetic events can be determined by their mutual relationships. The diagenetic sequence of the study area's Shaximiao Formation Reservoirs is gypsum cementation → chlorite cementation → feldspar dissolution → quartz overgrowth → kaolinite precipitation → laumontite cementation → laumontite dissolution → carbonate cementation → pyrite cementation. Combined with multiple indicators and industry standards, the reservoirs are classified into the syndiagenetic stage, early diagenetic stage, and middle diagenetic stage A (Figure 11).

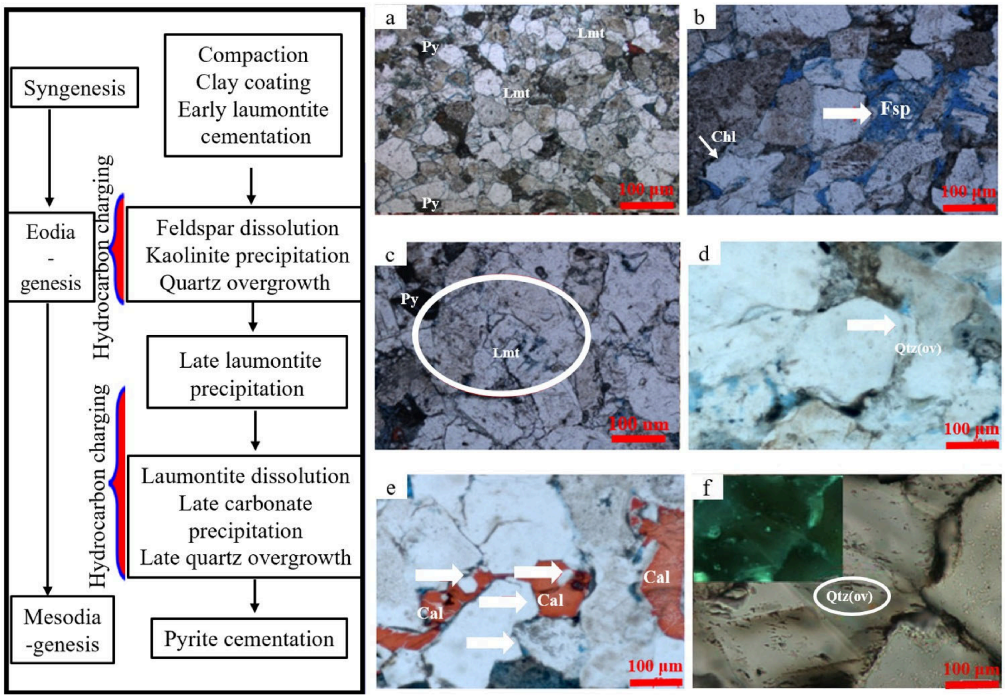


Figure 11. Diagenetic evolution and microscopic characteristics of the First Member of the Shaximiao Formation Reservoirs. (**a**) Well Zhongqian 1, 2660.94 m, laumontite cementation; (**b**) Well Jinhua 9, 2218.59 m, feldspar dissolution; (**c**) Well Jiantan 1, 1924.01 m, laumontite filling feldspar dissolved pores; (**d**) Well Jiantan 1, 1677.80 m, quartz overgrowth; (**e**) Well Jiantan 1, 1805.50 m, calcite cementation; (**f**) Well Jiantan1, 1805.50 m, quartz overgrowth. Calcite—Cal, quartz—Qtz, quartz overgrowth—Qtz(ov), feldspar—Fsp, laumontite—Lmt, pyrite cementation—Py, chlorite cementation—Chl. Eodia—eodiagenesis (shallow-burial early diagenesis), Mesodia—mesodiagenesis (moderate-burial diagenesis) [36].

Combined with diagenetic stages, mineral assemblages and variations in fluid activity, the diagenetic environments of Shaximiao Formation Reservoirs in the study area are subdivided into three types. From the syndiagenetic stage to early diagenetic stage A, the area is dominated by compaction. The diagenetic system remains relatively closed with weak exchange of external fluids and substances [36]. Continuous mechanical compaction squeezes mineral grains and reduces primary pores, which acts as the main cause for the deterioration of reservoir physical properties.

From early diagenetic stage B to the early middle diagenetic stage, the diagenetic system gradually evolves from closed to semi-open. Fluid circulation within formations is limited and allochthonous material supply is scarce. Compaction keeps intensifying, while calcite, laumontite, and clay minerals precipitate successively and fill intergranular pores, forming cementation-dominated diagenetic environments. Cementation further aggravates reservoir densification.

In the middle diagenetic stage, the diagenetic system turns fully open. Tectonic activities drive upward migration of deep organic acidic fluids along faults and unconformities, with well-defined fluid sources and migration pathways. Water–rock reactions between acidic fluids and reservoir minerals trigger extensive dissolution, resulting in dissolution-modified diagenetic environments. The evolutionary processes of different diagenetic types are systematically interpreted based on petrological characteristics and fluid evolution mechanisms.

5.1.1. Compaction-Dominated Diagenetic Environment

The syndiagenetic stage refers to the period after sediment deposition but before the sediment is completely covered by younger deposits and isolated from water [10–14], under paleo-normal temperature conditions (Figures 11 and 12). Terrestrial clastic sediments were transported by rivers, and elements most abundant in fresh water, such as Fe and Mn, precipitated in pore spaces. Rock consolidation was extremely weak, and abundant primary intergranular pores developed. The main diagenetic processes during this stage included hydration of aluminosilicate framework grains and synsedimentary volcanic materials, and formation of early clay mineral rims.

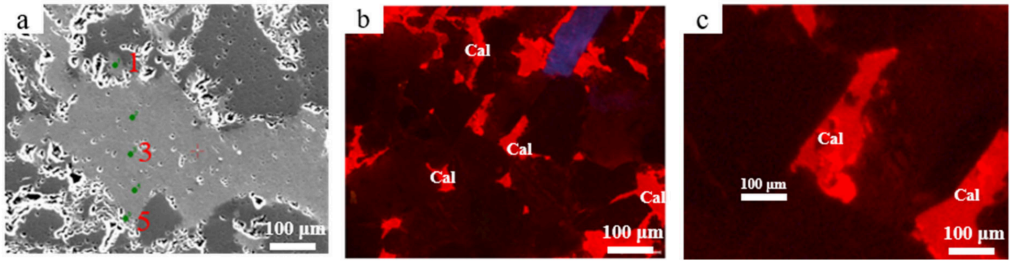


Figure 12. Microscopic characteristics of carbonate cements in the Shaximiao Formation. (**a**) Well Guankou 1, 2231.3 m, EPMA point location photograph, where numbers 1, 3, and 5 mark the EPMA test spots for elemental composition analysis; (**b**) Well Jinqian 7, 974.5 m, cathodoluminescence image showing intense red and orange–red luminescence of calcite cement; (**c**) Well Jinqian 7, 975.1 m, cathodoluminescence image showing intense red and orange–red luminescence of calcite cement. Calcite—Cal.

Early diagenetic stage A is characterized by complex diagenetic processes and represents a key period of reservoir pore loss. As the primary factor destroying pores in the Shaximiao Formation Reservoirs, compaction causes a total porosity reduction of 23.34%. Aluminosilicate and volcanic materials hydrated, supplying metal ions to diagenetic fluids [8–12]. Under acidic conditions, clay matrix altered to kaolinite; in high-pH environments, early calcite cementation formed poikilitic calcite. In sandstones with igneous fragments, hydration-induced alkaline fluids caused albitization and poikilitic laumontite precipitation.

Compaction rapidly reduces primary intergranular pores, which is particularly prominent in intervals lacking early cements. It tends to cause grain deformation and point contacts, accompanied by the formation of pore-lining chlorite. Well-developed chlorite coatings effectively protect primary pores, weaken the pore destruction caused by compaction, and mitigate the loss of initial porosity. Sandstones with abundant plastic grains are prone to rapid densification, which further inhibits subsequent chemical diagenesis. Early poikilitic calcite and chlorite can improve the compaction resistance of rocks, and thick chlorite rims play a vital role in preserving primary pores. Different from compaction, cementation is a secondary factor for reservoir pore loss. It mainly includes calcite cementation, siliceous cementation, and authigenic clay mineral cementation, resulting in a total porosity reduction of 9.12%. After the invasion of acidic fluids, feldspar is dissolved, and kaolinite as well as authigenic quartz precipitate simultaneously. Meanwhile, the reservoir begins to experience early hydrocarbon charging. Dissolution of feldspar and laumontite serves as the main pore-increasing process, which raises the porosity by 5.26% and 4.32%, respectively.

5.1.2. Cementation-Dominated Diagenetic Environment

During early diagenetic stage B, the paleotemperature ranged from 65 °C to 85 °C, corresponding to vitrinite reflectance (Ro) values of 0.35%–0.5% [37]. The rock is further compacted, with grains in point-line contact, and chemical diagenesis becomes more

significant. Due to extensive expulsion of pore fluids during early diagenetic stage A, hydration and a small amount of organic acids expelled during the low-maturity stage of organic matter cause dissolution of detrital grains such as feldspar, supplying Ca^{2+}, Mg^{2+}, K^{+}, Na^{+}, Fe^{2+}, and other ions to diagenetic fluids. Montmorillonite begins to transform into illite via illite/smectite mixed layers, releasing Na^{+}, Ca^{2+}, Fe^{2+}, Mg^{2+}, and Si^{4+} into pore fluids.

As a result, elevated concentrations of Ca^{2+}, Mg^{2+}, K^{+}, Na^{+}, Fe^{2+}, and other cations in diagenetic fluids lead to precipitation of authigenic quartz [38], quartz overgrowth, carbonate minerals, and other authigenic phases associated with burial diagenesis (Table 1). Hydrocarbon charging continues during this stage, and dissolution generates secondary dissolved pores. Accompanying these processes, late-stage laumontite precipitates, and partial dissolution of laumontite forms intercrystalline-dissolved pores (Figures 11–13).

Table 1. EPMA results of the sample from Well Guankou1 at 2231.3 m (wt%).

Component	Guankou1-1, 2231.3 m	Guankou1-2, 2231.3 m	Guankou1-3, 2231.3 m	Guankou1-4, 2231.3 m	Guankou1-5, 2231.3 m
Na_2O	0.089	0.017	0.016	0.003	0.102
K_2O	0.343	0.008	0.005	0.01	1.857
MnO	0.078	0.153	0	0	0.015
SiO_2	2.581	1.009	0.948	0.914	10.794
MgO	0.344	0.406	0.52	0.577	0.708
CaO	55.989	58.674	60.721	57.746	44.292
FeO	0.24	0.062	0.044	0.075	0.999
SrO	0.139	0	0.134	0.116	0
Al_2O_3	0.396	0.017	0.016	0	3.944
Total	60.199	60.344	62.404	59.44	62.712

Note: The measuring points correspond to the labeled positions in the SEM image.

Carbonate components are adequately supplied from two sources: detrital carbonate fragments and carbonate minerals within interbedded mudstones. Significant regional fluid heterogeneity exists, with higher carbonate cement contents in reservoirs in the western Sichuan Basin compared to the central Sichuan Basin. This indicates that carbonate rock fragments in the provenance system supply large amounts of carbonate components to diagenetic fluids, further promoting calcite cementation in sandstones. Vertically, a large number of carbonate minerals are developed in the mudstone layers at the base of thick sandstone successions. These carbonate minerals dissolve during diagenesis and release carbonate components into the pore fluid system of adjacent sandstones, eventually forming extensive tight calcite cemented layers at the sandstone–mudstone transition zones. Electron probe microanalysis results show that calcite cements in the study area are generally characterized by low Fe and Mn contents. Except for CaO, the contents of other major elements are all less than 1%, indicating a simple composition and a dominantly internal fluid source (Figure 13a).

The development characteristics of siliceous cementation in the study area are closely related to diagenetic fluid evolution and the state of the diagenetic system (Figure 13b). When the siliceous cement content is less than 2%, quartz overgrowth can effectively strengthen the rock framework and resist porosity reduction caused by compaction, showing a positive correlation with reservoir porosity. As the siliceous cement content continue to increase, the cement fills pores in the form of pore-throat blocking aggregates, leading to a rapid decrease in reservoir porosity. Although quartz is a stable mineral, organic acid fluids during diagenesis can significantly increase the quartz dissolution rate. Therefore, slight dissolution is commonly observed at the edges of quartz overgrowths in the Shaximiao Formation sandstones. Overall, the siliceous cement content in the study area is

generally less than 2.5%, which is relatively low, but it predominantly plays a destructive role in pores.

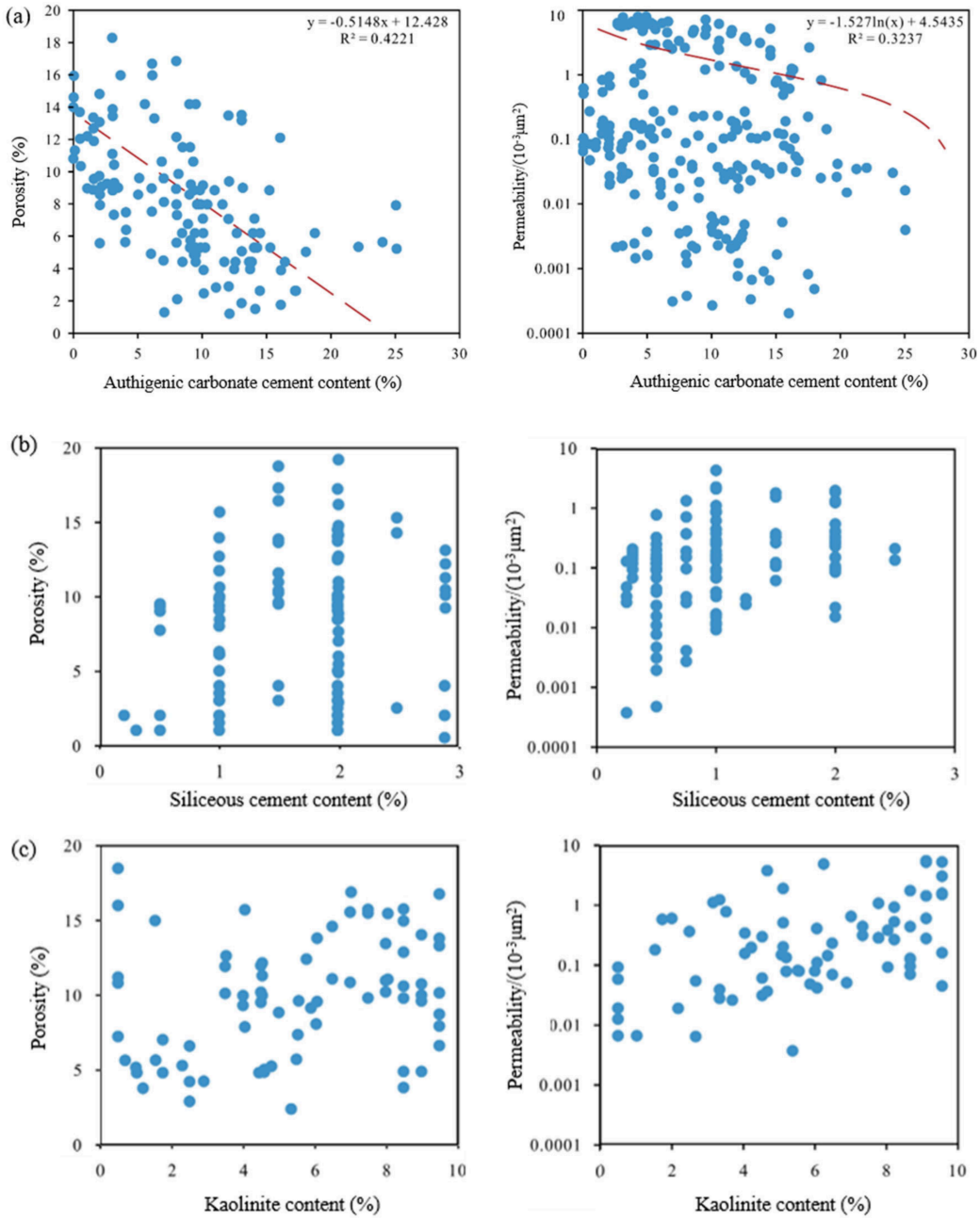


Figure 13. Relationships between authigenic cement contents and porosity and permeability in the Shaximiao Formation. (**a**) Cross plots of porosity and permeability versus authigenic carbonate cement content. Porosity has a linear negative correlation with authigenic carbonate cement, while permeability shows a logarithmic negative correlation with it. Carbonate cement fills intergranular pores and significantly deteriorates reservoir physical properties; (**b**) Cross plots of porosity and permeability versus siliceous cement content. Porosity and permeability first rise and then show scattered distribution, and siliceous overgrowth reduces pore space; (**c**) Cross plots of porosity and permeability versus kaolinite clay mineral content. No obvious monotonic correlation exists between porosity and permeability in kaolinite-developed zones; kaolinite fills pores yet retains partial tiny intergranular pores.

The development patterns of authigenic clay minerals further reveal the semi-open nature of the diagenetic system and fluid migration characteristics in the study area

(Figure 13c). Authigenic clay minerals can significantly increase the tortuosity of pore throats, greatly reducing reservoir permeability. The kaolinite content in the study area is much higher than that of siliceous cement. The core reason is that the diagenetic fluids have long been undersaturated with respect to silica: large amounts of silica released by feldspar dissolution are transported out of the reservoir system with pore fluids in an open-to-semi-open diagenetic system, making it difficult to form siliceous cement in situ. In contrast, kaolinite produced by feldspar hydrolysis is difficult to migrate with fluids and remains continuously enriched in reservoir pores. This mineral assemblage feature fully confirms that during the large-scale development of kaolinite, the diagenetic system of the Shaximiao Formation Reservoirs was generally semi-open, with obvious fluid exchange and material migration characteristics.

5.1.3. Dissolution-Modified Diagenetic Environment

In the study area, this stage is characterized by paleotemperatures ranging from 85 °C to 128 °C and vitrinite reflectance (Ro) values of 0.5%–1.31% [37], indicating that organic matter is in the mature stage. Rock consolidation is relatively high, and the influence of compaction diminishes. During middle diagenetic stage A, organic matter enters the mature stage and generates abundant organic acids, rendering pore fluids weakly acidic. The dominant diagenetic process is the dissolution of unstable components, which corrodes mineral grains and readily soluble cements, effectively improving reservoir pore space (Figure 14).

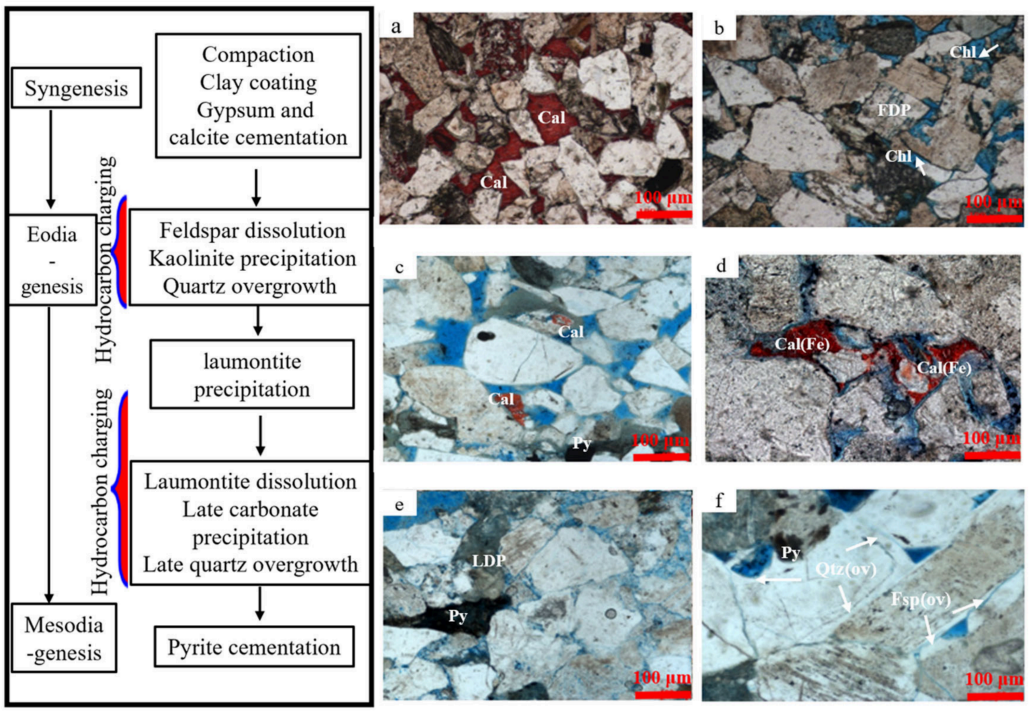


Figure 14. Diagenetic evolution and microscopic characteristics of the Second Member of the Shaximiao Formation Reservoirs. (**a**) Well Qiulin 16, 2234.39 m, calcite cementation; (**b**) Well Qiulin 18, 2085.94 m, feldspar dissolution; (**c**) Well Jinqian 3, 2153.07 m, clay coating and early calcite cementation; (**d**) Well Jinqian 7, 1758.65 m, iron-bearing calcite cementation; (**e**) Well Jinqian 3, 2148.8 m, laumontite dissolution; (**f**) Well Jinqian 3, 2148.80 m, quartz overgrowth and feldspar overgrowth. Calcite—Cal, quartz—Qtz, quartz overgrowth—Qtz(ov), feldspar—Fsp, laumontite—Lmt, feldspar dissolution pores—FDP, laumontite dissolution pores—LDP, pyrite cementation—Py, chlorite cementation—Chl. Eodia-eodiagenesis (shallow-burial early diagenesis), Mesodia—mesodiagenesis (moderate-burial diagenesis) [36].

Differences in reservoir evolution between the First and Second Members of the Shaximiao Formation were mainly formed during the early diagenetic stage. The First Member of the Shaximiao Formation experienced early laumontite cementation, whereas the Second Member of the Shaximiao Formation was dominated by gypsum and early calcite cementation. Intense dissolution greatly improves reservoir physical properties. In the Shaximiao Formation, secondary pores are mainly formed by the dissolution of feldspar, laumontite, and anhydrite. Both feldspar dissolution and laumontite dissolution show a positive correlation with porosity, which indicates that dissolution facilitates pore development and governs the distribution of high-quality reservoirs. The enrichment of laumontite in the study area is closely related to the development of intermediate-acid volcanic clastics. The albitization of plagioclase provides the main material source for late-metasomatic laumontite. Electron probe test results show that laumontite in the study area is mainly composed of Si, Al, and Ca, with minor trace elements such as Na, K, and Fe (Table 2). Genetic analysis indicates that laumontite commonly replaces plagioclase and is closely associated with albite, showing a unified genetic relationship. During diagenesis, plagioclase undergoes albitization accompanied by mineral component reorganization and ionic migration in diagenetic fluids, which ultimately promotes the precipitation of laumontite (Figure 15).

Table 2. EPMA results of laumontite (wt%).

Component	Jiantan1-1, 1929.12 m	Jiantan1-2, 1924.01 m	Jiantan1-3, 1924.00 m	Jinqian7-4, 1785.23 m	Jinqian7-5, 1785.23 m
Na_2O	0.183	0.183	0.193	0.21	0.283
K_2O	0.148	0.062	0.105	0.13	0.214
MnO	0.006	0.01	0	0.006	0.232
SiO_2	52.757	52.256	53.615	52.781	47.563
MgO	0.015	0.001	0.04	0.014	1.851
CaO	11.982	12.061	12.03	12.147	8.393
FeO	0.048	0.079	0.163	0.06	5.872
Al_2O_3	20.367	20.345	20.464	20.692	19.118

Note: The content of SrO is below the detection limit of electron probe microanalysis and thus recorded as 0. All samples were obtained from core samples of the Shaximiao Formation.

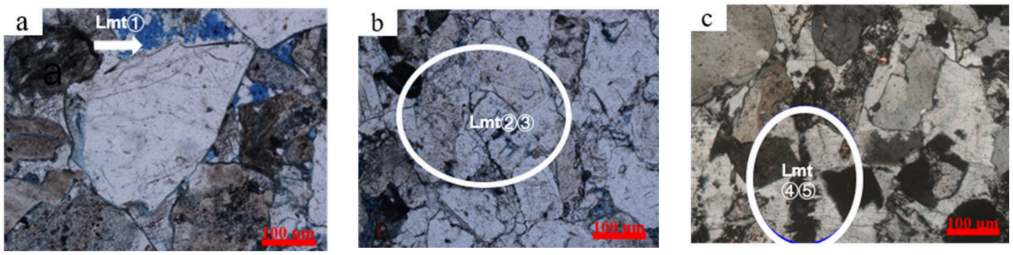


Figure 15. Microscopic characteristics of laumontite and EPMA measuring points in the Shaximiao Formation. (**a**) Well Jiantan 1, 1929.12 m, Point 1 shows differential dissolution of laumontite; (**b**) Well Jiantan 1, 1924.01 m, Points 2 and 3 show developed laumontite; (**c**) Well Jinqian 7, 1785.23 m, Points 4 and 5 show laumontite associated with albite. Laumontite—Lmt.

Feldspar dissolution, clay mineral evolution, and the open–closed state of the diagenetic system are strongly coupled, jointly controlling mineral assemblages and pore development in reservoirs. In a relatively closed diagenetic system, quartz and K-feldspar constitute the dominant stable framework minerals. Early dissolution of unstable plagioclase generates abundant secondary pores and leaves residual partially dissolved feldspar grains. Early sediments and contemporaneous volcanic clastics are rich in smectite and contain only a small amount of illite/smectite mixed layers with low illite content, alongside

kaolinite derived from feldspar dissolution. Acidic fluids serve as the key driving force for the alteration of aluminosilicate minerals. Extensive dissolution of unstable feldspar by early acidic fluids makes kaolinite the dominant clay mineral during burial diagenesis. Excessively high initial smectite content can consume active ions in the diagenetic system and inhibit K-feldspar dissolution and kaolinite illitization during late diagenesis.

In a relatively open diagenetic system, external fluids continuously supply potassium ions, which alter the evolutionary pathway of reservoir minerals together with early unstable feldspar dissolution and kaolinite precipitation. Extraneous potassium sources independent of K-feldspar dissolution can break the kinetic barrier of mineral transformation and significantly promote feldspar dissolution. Combined with the tectonic and sedimentary background of the Shaximiao Formation, the acidic fluids responsible for feldspar dissolution are mainly organic acids derived from hydrocarbon expulsion of the Xujiahe, Lianggaoshan, and Daanzhai source rocks, with the involvement of extra low-salinity surface-derived fluids. After being dissolved by acidic fluids, feldspar undergoes component redistribution, forming in situ kaolinite precipitation and quartz overgrowth, which constitutes the typical dissolution–cementation diagenetic assemblage in the study area.

5.2. Diagenetic Environments Controlling Porosity Evolution

Differences in reservoir physical properties caused by diagenesis are referred to as diagenetic heterogeneity, which is particularly prominent in the Shaximiao Formation Reservoirs and results in strong vertical and lateral reservoir variations.

Taking the interval from 2224 m to 2234 m in Well Qiulin 16 as an example: At the top, micrographs show abundant matrix and mica, resulting in poor reservoir physical properties, accompanied by well-developed carbonate cementation. The middle part corresponds to a scoured surface within stacked thick sand bodies, where reservoir physical properties are significantly reduced. Near the basal scoured surface, high matrix content and intense carbonate cementation lead to further deterioration of physical properties. Taking the interval from 2234 m to 2246 m in Well Qiulin 16 as an example: at 2234 m, although matrix content is low and the sandstone is relatively clean, extensive carbonate cementation results in poor pore development (Figure 16).

At the middle interval of 2239.74 m, despite relatively high carbonate cement content, partial dissolution of carbonate cements leads to well-developed secondary pores. At the bottom of 2244.06 m, near the base of the thick sand body, high matrix content and widespread carbonate cementation make the sandstone extremely tight with almost no pores, and porosity and permeability reach their lowest values (Figure 17).

Differences in sand body stacking patterns among sedimentary facies strengthen the reservoir heterogeneity of the fluvial–deltaic Shaximiao Formation. Lateral and vertical variations in sedimentary facies, together with different provenance conditions between central and western Sichuan, cause marked differences in rock composition and texture. Reservoir heterogeneity is further reflected in differentiated diagenetic evolution controlled by sedimentary structures. Affected by compaction, cementation, and dissolution, different positions within sand bodies develop distinct reservoir characteristics: the middle of thick sand bodies favors dissolution and forms relatively high-quality reservoirs; the base is commonly tightened by carbonate cementation; and the top adjacent to mudstone tends to become tight owing to strong compaction, caused by finer grains and higher contents of soft fragments.

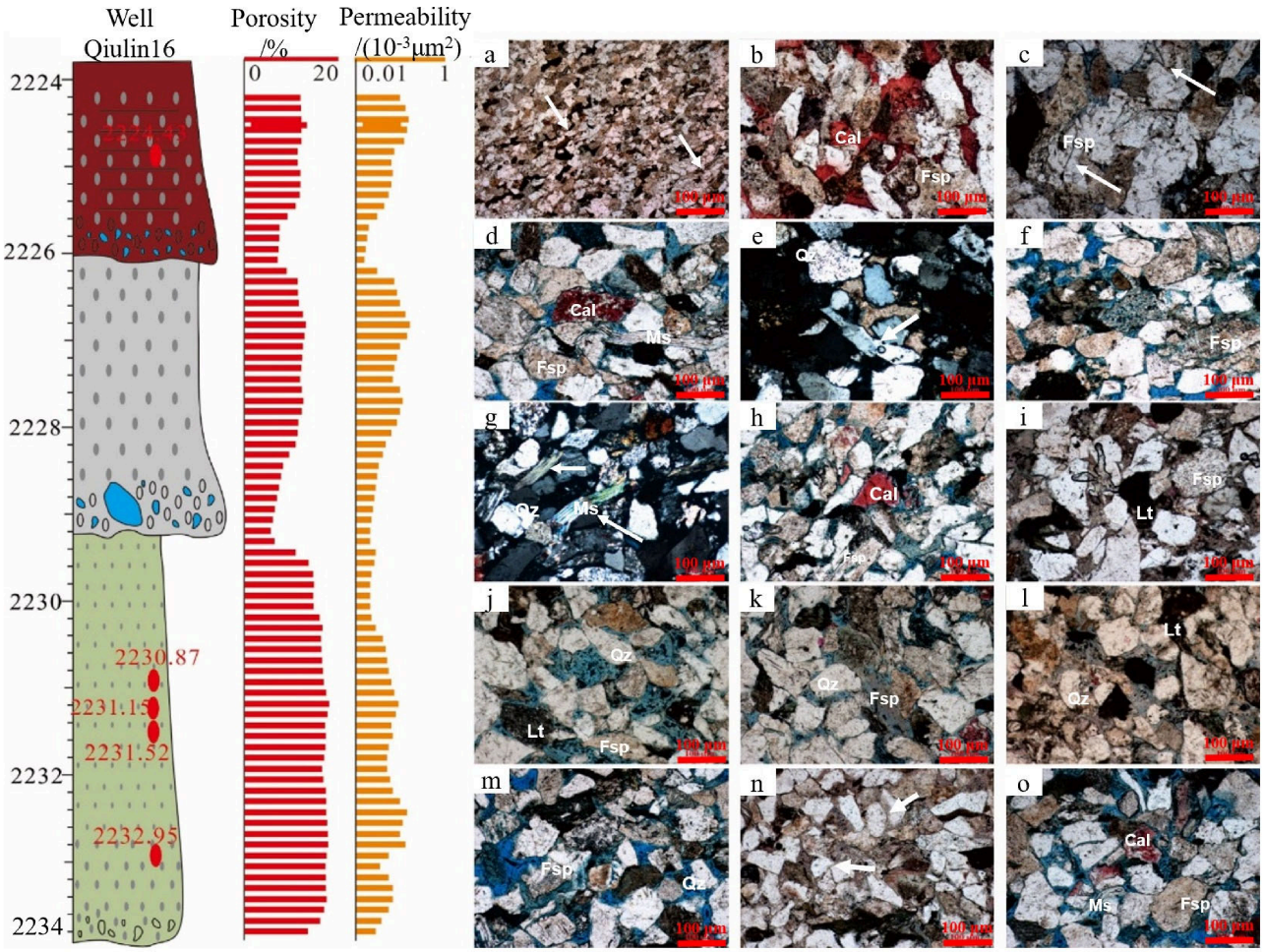


Figure 16. Stratigraphic column and reservoir microphotographs of the Shaximiao Formation in Well Qiulin 16. Well Qiulin 16, 2224.43 m, thin sections (**a**–**c**) show tight grain contacts with calcite cementation; compaction caused deformation of mica and lithic fragments, and feldspar grain fractures are observed in thin section (**c**). At 2230.87 m, thin sections (**d**–**f**) exhibit compaction-induced deformation of lithic fragments and mica under both plane-polarized light and cross-polarized light, along with minor primary intergranular pores and slight intragranular dissolution of feldspar. At 2231.15 m, thin sections (**g**–**i**) show tight grain contacts with minor calcite cementation. At 2231.52 m, thin sections (**j**–**l**) show minor primary intergranular pores with predominantly linear grain contacts. At 2232.95 m, thin sections (**m**–**o**) show predominantly linear grain contacts, with calcite cementation and clay minerals present. Calcite—Cal, quartz—Qtz, quartz overgrowth—Qtz(ov), feldspar—Fsp, lithic fragments—Lt, Mica—Ms.

Combined with the above observations from Well Qiulin 16, the diagenetic evolution is further discussed from the perspectives of diagenetic environment, fluid properties, system openness, and fluid sources. The study area belongs to a shallow-to-medium burial diagenetic setting. Vertically differentiated diagenetic environments occur within sand bodies, and provenance differences between central Sichuan and western Sichuan aggravate regional diagenetic variations. Two types of diagenetic fluids control reservoir evolution: alkaline fluids dominate at the top, bottom, and scoured surfaces of sand bodies and trigger extensive carbonate cementation, while acidic fluids mainly concentrate in the middle of sand bodies and dissolve cements and feldspar to form secondary pores. The diagenetic system is generally semi-closed. The middle part of thick sand bodies features good connectivity and a relatively open system, facilitating fluid migration and dissolution. In contrast, the top and bottom of sand bodies are blocked by mudstone and tight rocks, forming semi-closed-to-closed systems where cement accumulation and compaction jointly

result in tight reservoirs. Diagenetic fluids were mainly derived from primary alkaline formation water of sedimentary stage and secondary acidic fluids generated by organic matter maturation. The coupling of sedimentary conditions and diagenetic processes ultimately leads to strong reservoir heterogeneity of the Shaximiao Formation, with relatively good physical properties in the middle of sand bodies and tight intervals at the top and bottom.

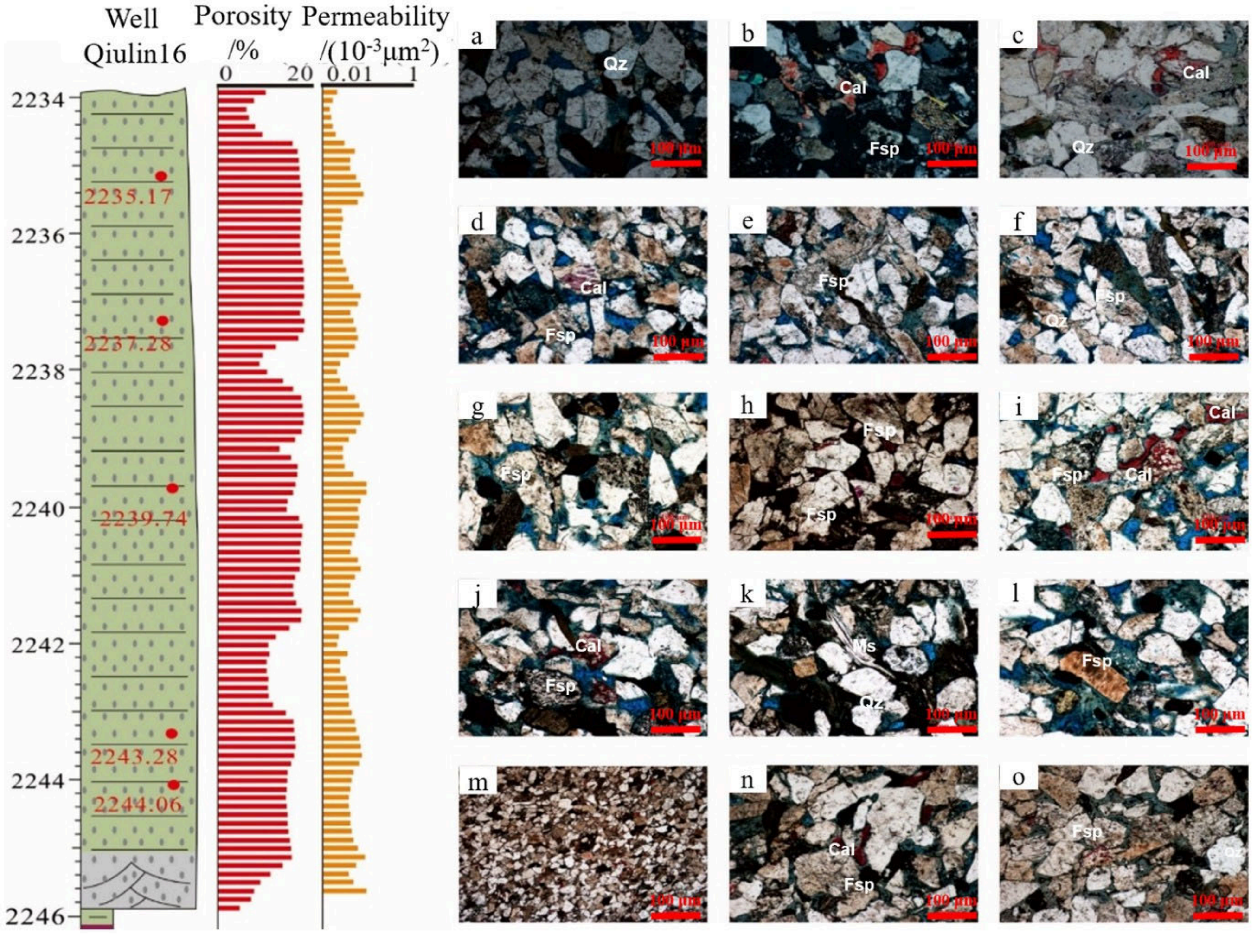


Figure 17. Stratigraphic column and reservoir microphotographs of the Shaximiao Formation, Well Qiulin 16. Well Qiulin 16. At 2235.17 m, thin sections (**a**–**c**) show calcite cementation. At 2237.28 m, thin sections (**d**–**f**) exhibit minor dissolution of feldspar and carbonate cements. At 2239.74 m, thin sections (**g**–**i**) contain a small amount of calcite cement with visible calcite dissolution. At 2243.28 m, thin sections (**j**–**l**) have a few primary pores, with secondary pores being dominant. At 2244.06 m, thin sections (**m**–**o**) show minor calcite cement. Calcite—Cal, quartz—Qtz, quartz overgrowth—Qtz(ov), feldspar—Fsp, lithic fragments—Lt, Mica—Ms.

In a relatively closed diagenetic system, reservoirs are dominated by quartz and K-feldspar, with secondary pores mainly derived from plagioclase dissolution. Acidic fluids promote aluminosilicate dissolution and form kaolinite-rich clay assemblages, while high smectite content reduces K-feldspar consumption and inhibits kaolinite illitization. In an open diagenetic system, exogenous K^+ changes the dissolution–precipitation equilibrium of K-feldspar, lowers reaction kinetic barriers, and controls the final mineral and pore distribution (Figure 18).

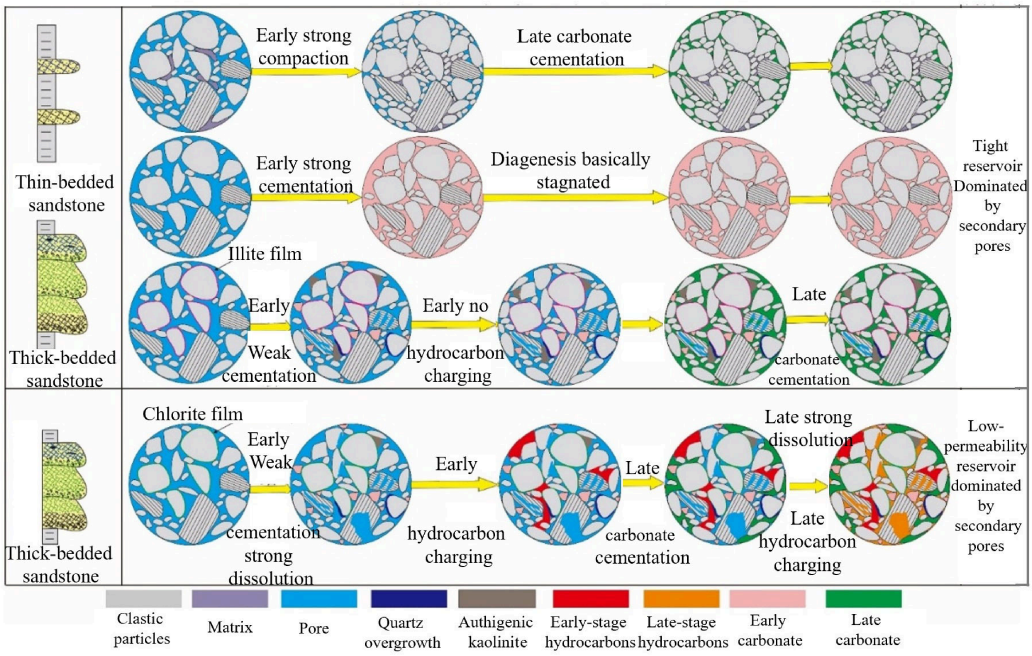


Figure 18. Diagenetic modification and evolution model of the Shaximiao Formation Reservoirs.

The reservoir evolutionary model of the Shaximiao Formation in central and western Sichuan shows obvious heterogeneity. Strong carbonate cementation commonly develops in thin sand bodies and the margins of thick sand bodies, forming calcareous tight intervals. In the center of thick sand bodies, controlled by early clay coating, weak cementation and dissolution, hydrocarbon charging determines reservoir quality: reservoirs without hydrocarbon charging become tightly compacted, whereas charged intervals remain effective. Spatially, reservoirs near the Longmen Mountains feature intensive calcite cementation, central Sichuan develops widespread laumontite cementation, and transitional zones are characterized by effective laumontite dissolution.

6. Conclusions

Based on thin-section observation, scanning electron microscopy, cathodoluminescence, electron probe, fluid inclusion, and physical property tests, this paper systematically investigates the diagenetic environment of the Shaximiao Formation Reservoirs, and the main conclusions are as follows:

(1) Basic reservoir characteristics. The Shaximiao Formation in the Sichuan Basin is characterized by typical low-permeability tight reservoirs, which are mainly composed of lithic arkose, followed by feldspathic litharenite and a small amount of arkose. Authigenic minerals such as laumontite, calcite, quartz overgrowth, feldspar overgrowth, and clay minerals are widely developed. The reservoir spaces primarily include primary pores, feldspar dissolution pores, and laumontite dissolution pores.

(2) Densification mechanism. Compaction is the dominant factor causing porosity reduction, followed by cementation, while the dissolution of feldspar and laumontite effectively improves reservoir porosity. The Shaximiao Formation Reservoirs have experienced two-stage densification. The first densification was caused by compaction and cementation during the early and middle diagenetic stages, and the second densification resulted from widespread authigenic mineral filling in the late diagenetic stage.

(3) Sedimentary and diagenetic controlling factors. Diagenetic environments and material sources jointly dominate the diagenetic assemblages and physical properties

of the reservoirs. Mudstone and carbonate rock fragments from western Sichuan provide essential materials for calcite cementation. The development of intermediate-acid pyroclastics and plagioclase albitization jointly promote laumontite enrichment. Feldspar dissolution induced by infiltration of low-salinity surface-derived fluids and upward migration of organic acids along faults promotes the generation of kaolinite and quartz overgrowths. The brackish diagenetic environment under arid climate conditions favors the development of early diagenetic gypsum, which is finally transformed into anhydrite through burial dehydration.

Author Contributions: Conceptualization, S.L.; methodology, J.T.; software, S.L. and C.L.; formal analysis, J.T.; investigation, C.L.; resources, S.L.; writing—original draft, J.T.; funding acquisition, C.L. All authors have read and agreed to the published version of the manuscript.

Funding: This work was supported by the Natural Science Foundation of Chongqing, China (Grant No. CSTB2022NSCQ-MSX1402), the Project of Science and Technology Research Program of the Chongqing Municipal Education Commission, China (Grant No. KJQN202301549), the Open Fund of SINOPEC Key Laboratory of Acid Gas Field Development (Grant No. 31300027-25-ZC0613-0029), and the Open Fund of SINOPEC Key Laboratory of Marine Oil and Gas Reservoir Development (Grant No. 33550000-26-ZC0609-0006).

Data Availability Statement: The data presented in this study are available on request from the corresponding author due to industrial confidentiality restrictions.

Conflicts of Interest: The authors declare no conflict of interest.

References

1. Shanley, K.W.; Cluff, R.M.; Robinson, J.W. Factors controlling prolific gas production from low-permeability sandstone reservoirs: Implications for resource assessment, prospect development, and risk analysis. *AAPG Bull.* **2004**, *88*, 1083–1121. [CrossRef]
2. Milliken, K.L.; Curtis, M.E. Imaging pores in sedimentary rocks: Foundation of porosity prediction. *Mar. Pet. Geol.* **2016**, *73*, 590–608. [CrossRef]
3. Crundwell, F.K. On the mechanism of the dissolution of quartz and silica in aqueous solutions. *ACS Omega* **2017**, *2*, 1116–1127. [CrossRef] [PubMed]
4. Silva, H.S.; Sodero, A.C.; Korb, J.-P.; Alfarra, A.; Giusti, P.; Vallverdu, G.; Bégué, D.; Baraille, I.; Bouyssiere, B. The role of metalloporphyrins on the physical-chemical properties of petroleum fluids. *Fuel* **2017**, *188*, 374–381. [CrossRef]
5. Berra, F.; Azmy, K.; Della Porta, G. Stable-isotope and fluid inclusion constraints on the timing of diagenetic events in the dolomitized Dolomia Principale inner platform (Norian, Southern Alps of Italy). *Mar. Pet. Geol.* **2020**, *121*, 104615. [CrossRef]
6. Kassem, A.A.; Hussein, W.S.; Radwan, A.E.; Anani, N.; Abioui, M.; Jain, S.; Shehata, A.A. Petrographic and diagenetic study of siliciclastic Jurassic sediments from the northeastern margin of Africa: Implications for reservoir quality. *J. Pet. Sci. Eng.* **2021**, *200*, 108340. [CrossRef]
7. Teixeira, C.A.S.; Sawakuchi, A.O.; Bello, R.M.S.; Nomura, S.F.; Bertassoli, D.J.; Chamani, M.A. Fluid inclusions in calcite-filled opening fractures of the Serra Alta Formation reveal paleotemperatures and composition of diagenetic fluids percolating Permian shales of the Paraná Basin. *J. S. Am. Earth Sci.* **2018**, *84*, 242–252.
8. Bradbury, H.J.; Turchyn, A.V. Calcium isotope fractionation in sedimentary pore fluids from ODP Leg 175: Resolving carbonate recrystallization. *Geochim. Cosmochim. Acta* **2018**, *236*, 121–139. [CrossRef]
9. Pichat, A.; Hoareau, G.; Callot, J.P.; Ringenbach, J.C. Diagenesis of Oligocene continental sandstones in salt-walled mini-basins—Sivas Basin, Turkey. *Sediment. Geol.* **2016**, *339*, 13–31.
10. Bjørlykke, K. Relationships between depositional environments, burial history and rock properties: Some principal aspects of diagenetic process in sedimentary basins. *Sediment. Geol.* **2014**, *301*, 1–14. [CrossRef]
11. Deng, T.; Li, Y.; Wang, Z.J.; Yu, Q.; Dong, S.; Yan, L.; Hu, W.; Chen, B. Geochemical characteristics and organic matter enrichment mechanism of black shale in the Upper Triassic Xujiahe Formation in the Sichuan Basin: Implications for paleoweathering, provenance, and tectonic setting. *Mar. Pet. Geol.* **2019**, *109*, 698–716. [CrossRef]
12. Alam, K.; Abdullatif, O.; El-Husseiny, A.; Babalola, L. Depositional and diagenetic controls on reservoir heterogeneity and quality of the Bhuban Formation, Neogene Surma Group, Srikail Gas Field, Bengal Basin, Bangladesh. *J. Asian Earth Sci.* **2022**, *223*, 104985. [CrossRef]

13. Worden, R.H.; Benshatwan, M.S.; Potts, G.J.; Elgarmadi, S.M. Basin-scale fluid movement patterns revealed by veins: Wessex Basin, UK. *Geofluids* **2015**, *16*, 149–174.
14. Xi, K.; Cao, Y.; Jahren, J.; Zhu, R.; Bjørlykke, K.; Zhang, X.; Cai, L.; Hellevang, H. Quartz cement and its origin in tight sandstone reservoirs of the Cretaceous Quantou Formation in the southern Songliao Basin, China. *Mar. Pet. Geol.* **2015**, *66*, 748–763. [CrossRef]
15. Katagiri, J.; Kimura, S.; Noda, S. Significance of shape factor on permeability anisotropy of sand: Representative elementary volume study for pore-scale analysis. *Acta Geotech.* **2020**, *15*, 2195–2203. [CrossRef]
16. Kashif, M.; Cao, Y.C.; Yuan, G.H.; Asif, M.; Javed, K.; Mendez, J.N.; Khan, D.; Miruo, L. Pore size distribution, their geometry and connectivity in deeply buried Paleogene Es1 sandstone reservoir, Nanpu Sag, East China. *Pet. Sci.* **2019**, *16*, 981–1000. [CrossRef]
17. Qiao, J.; Zeng, J.; Chen, D.; Cai, J.; Jiang, S.; Xiao, E.; Zhang, Y.; Feng, X.; Feng, S. Permeability estimation of tight sandstone from pore structure characterization. *Mar. Pet. Geol.* **2022**, *135*, 105382. [CrossRef]
18. Bishop, J.W.; Osleger, D.A.; Montañez, I.; Sumner, D.Y. Meteoric diagenesis and fluid-rock interaction in the Middle Permian Capitan backreef: Yates Formation, Slaughter Canyon, New Mexico. *AAPG Bull.* **2014**, *98*, 1495–1519. [CrossRef]
19. Li, S.Y.; Tian, J.C.; Lin, X.B.; Yin, N.; Luo, C.; Yang, D. Reconstruction of the diagenetic environments of tight sandstone reservoirs: A case study from the Tengger Formation in the Baiyinchagan Sag, Erlian Basin, Northern China. *Lithosphere* **2022**, *2022*, 9220510. [CrossRef]
20. Jia, C.Z.; Zhao, W.; Song, Y.; Jiang, L.; Fu, X.; Cheng, L. Geological characteristics and accumulation mechanisms of conventional-tight transitional sandstone gas: A case study of the Xujiahe Formation to Shaximiao Formation in the Sichuan Basin. *Nat. Gas Ind.* **2025**, *45*, 53–65.
21. Wen, L.; Luo, B.; Wang, X.J.; Xie, J.; Ran, Q.; Pan, K.; Jin, Z.; Guan, X. New exploration fields and resource potential of continental tight oil and gas in Sichuan Basin. *Acta Pet. Sin.* **2025**, *46*, 77–88.
22. Zhang, D.W.; Yang, Y. Exploration potential and development direction of continental tight sandstone gas in the Sichuan Basin. *Nat. Gas Ind.* **2022**, *42*, 1–11.
23. Ma, X.H.; Yang, Y.; Wen, L.; Luo, B. Distribution and exploration direction of medium- and large-sized marine carbonate gas fields in Sichuan Basin, SW China. *Pet. Explor. Dev.* **2019**, *46*, 1–13. [CrossRef]
24. Zhao, M.; Guo, Z.Q.; Qing, H.; Zhang, L.L.; Liu, W. Application of casting thin section identification and microscopic image analysis technology for rocks. *West-China Explor. Eng.* **2009**, *21*, 66–68.
25. Yu, L.Z.; Lu, J. Basic principle and application of scanning electron microscope. *Exp. Sci. Technol.* **2019**, *17*, 85–93.
26. Wang, R.F.; Chen, M.Q. Quantitative analysis of porosity parameter evolution during reservoir sedimentary-diagenetic processes: A case study of Yan 25 and Zhuang 40 blocks in Ordos Basin. *Acta Geol. Sin.* **2007**, *81*, 1432–1438, 1451–1452.
27. Xu, N.C.; Shen, J.L.; Zhang, J. Application of X-ray diffraction, X-ray fluorescence spectrometry and electron probe microanalysis in mineral identification of basalt. *Rock Mineral Anal.* **2015**, *34*, 75–81.
28. Huang, S.J. Cathodoluminescence of carbonate minerals and its correlation with Fe and Mn contents. *Miner. Rocks* **1992**, *12*, 74–79.
29. Goldstein, R.H. Reequilibration of fluid inclusions in low-temperature calcium-carbonate cement. *Geology* **1986**, *14*, 792–795.
30. Goldstein, R.H. Fluid inclusions in sedimentary and diagenetic systems. *Lithos* **2001**, *55*, 159–193. [CrossRef]
31. Folk, R.L. The Distinction between Grain Size and Mineral Composition in Sedimentary-Rock Nomenclature. *J. Geol.* **1954**, *62*, 344–359. [CrossRef]
32. Folk, R.L. *Petrology of Sedimentary Rocks*; Hemphill Publishing Company: Austin, TX, USA, 1968.
33. Deville de Periere, M.; Mangenot, X.; Dyja-Person, V.; Aldhubaib, A. Sedimentology and diagenetic evolution of the Upper Permian Khuff Formation in Saudi Arabia. New perspectives from biostratigraphy, U/Pb geochronology and fluid inclusions. *Mar. Pet. Geol.* **2025**, *179*, 107462. [CrossRef]
34. Azmy, K.; Blamey, N.J.F. Source of diagenetic fluids from fluid-inclusion gas ratios. *Chem. Geol.* **2013**, *347*, 246–254. [CrossRef]
35. Bodnar, R.J. Revised equation and table for determining the freezing point depression of H_2O–NaCl solutions. *Geochim. Cosmochim. Acta* **1993**, *57*, 683–684.
36. Morad, S.; Ketzer, J.M.; De Ros, L.F. Spatial and temporal distribution of diagenetic alterations in siliciclastic rocks: Implications for mass transfer in sedimentary basins. *Sedimentology* **2002**, *47*, 95–120.
37. Wang, Y. *Evaluation of Exploration Targets for the Shaximiao Formation in Southern Sichuan*; Southwest Petroleum Institute: Chengdu, China, 2004.
38. Dove, P.M. The dissolution kinetics of quartz in aqueous mixed cation solutions. *Geochim. Cosmochim. Acta* **1999**, *63*, 3715–3727. [CrossRef]

Disclaimer/Publisher's Note: The statements, opinions and data contained in all publications are solely those of the individual author(s) and contributor(s) and not of MDPI and/or the editor(s). MDPI and/or the editor(s) disclaim responsibility for any injury to people or property resulting from any ideas, methods, instructions or products referred to in the content.